การศึกษาปฏิกิริยาการสลายไซโครเฮกเซน โดยใช้ตัวเร่งปฏิกิริยาโคบอลต์กัมมันต์เดี่ยว

THE STUDY OF CYCLOHEXANE CRACKING USING SINGLE-SITE COBALT HETEROGENEOUS CATALYSTS

ธีราภรณ์ กุระโท

สาธุ คูหาทัสนะดีกุล

อรุชา วรรธนเศรษฐ

โครงงานพิเศษนี้เป็นส่วนหนึ่งของการศึกษาตามหลักสูตร
ปริญญาวิทยาศาสตรบัณฑิต (เคมีอุตสาหกรรม)
ภาควิชาเคมี คณะวิทยาศาสตร์
สถาบันเทคโนโลยีพระจอมเกล้าเจ้าคุณทหารลาดกระบัง
ปีการศึกษา 2558

การศึกษาปฏิกิริยาการสลายไซโครเฮกเซน โดยใช้ตัวเร่งปฏิกิริยาโคบอลต์กัมมันต์เดี่ยว

THE STUDY OF CYCLOHEXANE CRACKING USING SINGLE-SITE COBALT HETEROGENEOUS CATALYSTS

ธีราภรณ์ กุระโท

สาธุ คูหาทัสนะดีกุล

อรุชา วรธนเศรษฐ

โครงงานพิเศษนี้เป็นส่วนหนึ่งของการศึกษาตามหลักสูตร

ปริญญาวิทยาศาสตรบัณฑิต (เคมีอุตสาหกรรม)

ภาควิชาเคมี คณะวิทยาศาสตร์

สถาบันเทคโนโลยีพระจอมเกล้าเจ้าคุณทหารลาดกระบัง

ปีการศึกษา 2558

THE STUDY OF CYCLOHEXANE CRACKING USING SINGLE-SITE COBALT HETEROGENEOUS CATALYSTS

TEERAPORN KURATO
SATU KUHATASANADEEKUL
ARUCHA WORATHNASETH

A SPECIAL PROJECT SUBMITTED IN PARTIAL FULFILLMENT OF
THE REQUIREMENT FOR
THE DEGREE OF BACHELOR OF SCIENCE (INDUSTRIAL CHEMISTRY)
DEPARTMENT OF CHEMISTRY, FACULTY OF SCIENCE
KING MONGKUT'S INSTITUTE OF TECHNOLOGY LADKRABANG
ACADEMIC YEAR 2015

Title	The study of cyclohexane cracking using single-site cobalt heterogeneous catalysts		
Students	Miss. Teeraporn	Kurato	55050691
	Mr. Satu	Kuhatasanadeekul	55050826
	Mr. Arucha	Worathanaseth	55050872
Degree	Bachelor of Science (Industrial Chemistry)		
Department	Chemistry		
Faculty	Science		
University	King Mongkut's Institute of Technology Ladkrabang (KMITL)		
Academic Year	2015		
Advisor	Dr. Kittisak Choojun		
Co-advisor	Assoc. Prof. Dr. Tawan Sooknoi		

Faculty of Science, King Mongkut's Institute of Technology Ladkrabang, has approved this special project submitted in partial fulfillment of the requirement for the degrees of Bachelor of Science (Industrial Chemistry) in academic year 2015.

Committees	Signatures
Asst. Prof. Dr. Sutha Sutthiruangwong Chairperson	
Dr. Karoon Sadorn Committee	Karoon Sadorn
Dr. Kittisak Choojun Committee and Advisor	
Assoc. Prof. Dr. Tawan Sooknoi Committee and Co-advisor	

Title	The study of cyclohexane cracking using single-site cobalt heterogeneous catalysts		
Students	Miss. Teeraporn	Kurato	Student ID 55050691
	Mr. Satu	Kuhatasanadeekul	Student ID 55050826
	Mr. Arucha	Worathanaseth	Student ID 55050872
Degree	Bachelor of Science (Industrial Chemistry)		
Department	Chemistry		
Faculty	Science		
University	King Mongkut's Institube of Technology Ladkrabang (KMITL)		
Academic Year	2015		
Advisor	Dr. Kittisak Choojun		
Co-advisor	Assoc. Prof. Dr. Tawan Sooknoi		

Abstract

The idea of using single-site catalysts is interested. This catalyst mimics the well-define active site as a homogeneous catalyst and can be easily removed from the reaction as a heterogeneous catalyst. They also showed the better activity as compared to non-single-site catalysts. In this research, the dehydrogenation of cyclohexane was investigated using single-site Co^{2+}/SiO_2 catalysts and non-single-site Co/SiO_2 catalyst. The catalysts preparation by electrostatic adsorption methodology using $[Co(bipy)_3](NO_3)_2$, $[Co(NH_3)_5Cl]Cl_2$, $[Co(NH_3)_6]Cl_3$ and $[Co(en)_2Cl_2]Cl$ as a precursor were compared impregnation method using $Co(NO_3)_2.6H_2O$ as a precursor. The reaction was carried out at various temperature and contract time. The dehydrogenation of cyclohexane yields cyclohexene, benzene, ethylene, ethane and 1,3-Butadiene. The result reveal that the non-single-site cobalt under using N_2 as a carrier gas has better cyclohexene selectivity, the non-reduced single-site cobalt has better activity, and the activity increases in the order : $[Co(bipy)_3](NO_3)_2 > [Co(NH_3)_5Cl]Cl_2 > [Co(NH_3)_6]Cl_3 > [Co(en)_2Cl_2]Cl > Co(NO_3)_2.6H_2O$. This is the result of the dispersion of cobalt. The product selectivity was modified by conversion.

Keywords : single-site cobalt

ACKNOWLEDGEMENTS

The authors take this opportunity to acknowledge advisors Dr. Kittisak Choojun and Assoc. Prof. Dr. Tawan Sooknoi, for the supervision, inspiration, suggestions, and encouragement throughout this research. In addition, We are grateful to thank Asst. Prof. Dr. Sutha Sutthiruangwong and Dr. Karoon Sadorn for serving as the committees and their valuable comments.

We would like to distribute a kindness thank to Catalytic Chemistry Research Unit members for their contribution of the ideas and facilities and most importantly their support.

Furthermore, we would like to appreciate the support from the Department of Chemistry, Faculty of Science, King Mongkut's Institute of Technology Ladkrabang for the advanced laboratory instruments, equipment, chemicals, and facilities.

Finally, the authors would like to gracefully thank to our parents and our friend, who give an encouragement. This thesis would not possible without them.

Teeraporn Kurato

Satu Kuhatasanadeekul

Arucha Worathanaseth

CONTENTS

CONTENTS (Continued)

CONTENTS (Continued)

LIST OF TABLES

LIST OF FIGURES

LIST OF FIGURES (Continued)

Page

CHAPTER 1
INTRODUCTION

1.1 Motivation

The global demand for hydrocarbon has been rising steadily because of the various applications. Olefin products are one of the most demanding hydrocarbons for polymer and fuel productions. Cracking of cyclohexane can generate benzene, ethylene, hydrogen and cyclohexene which are all valuable chemicals. Benzene has been used as an solvent and intermediate to synthesize several chemicals. Ethylene is predominantly used for polyethylene production. Hydrogen is considered as a clean energy. Cyclohexene is another chemicals used as an intermediate for the production of cyclohexanol, which is further dehydrogenated to give cyclohexanone. It is also a precursor for caprolactam in which could be converted to Nylon 6, a widely used in synthetic polymers. Cyclohexene deriving from dehydrogenation of cyclohexane is also an important precursor for adipic acid, maleic acid and dicyclohexyladipate syntheses. Furthermore, it is also used as a solvent.

Currently, cyclohexene is produced by the partial hydrogenation of benzene.[1] The alternative route is to use, the oxidative dehydrogenation of cyclohexane to produce cyclohexene, which has been intensively.[2-4] However, this routine exhibits low cyclohexene selectivity and produces significant amounts of CO_x. Another promising procedure is to use, the dehydrogenation of cyclohexane to cyclohexene which is one partway of cyclohexane cracking can be carried out without CO_x production. Moreover, hydrogen produced in this process is a desirable by-product, which can be used in several processes, such as, hydrocracking and hydrodesulfurization.

The dehydrogenation of cyclohexane using various metals loaded on various supports as a heterogeneous catalyst has been investigated. The examples are Pt/SiO_2 [5], Pt/Al_2O_3 [6], $Pt/MgAl(Sn)O_x$ [7], Pt and Pd on SC-CNT [8], NiP/Al_2O_3 [9] and Ni/Al_2O_3-TiO_2.[10] However, these catalysts generally produce coke during the reaction which reduces the number of active sites and causes the deactivation of catalysts.

In addition the use of, the noble metal, such as, Platinum (Pt), Palladium (Pd) is expensive. On the other hand, inexpensive metals that can activate C-H bond are Cobalt (Co), Ferrous (Fe) and Nickel (Ni).[11]

In order to reduce the deactivation of catalysts, the idea of single-site metal on support is introduced. This catalyst mimics the well-define active site as a homogeneous catalyst and can be easily removed from the reaction as a heterogeneous catalyst. Recently, single-site Co^{2+} [12] and single-site Zn^{2+} [13] on SiO_2 heterogeneous catalysts had been reported that they can activate C-H and H–H bond. They also showed the better activity, a high selectivity for propane dehydrogenation to propene, non-redox mechanism and less coke production.

Since cobalt shows C-H bond activation and it is considered as an inexpensive metal, we, thus, reason to study the use of single-site Co^{2+} on silica support for cracking of cyclohexane. The products distribution and their stability are investigated. The catalysts preparation are synthesized by electrostatic adsorption methodology. The effect of using different cobalt complexes as a precursor, including, $[Co(NH_3)_6]Cl_3$, $[Co(NH_3)_5Cl]Cl_2$, $[Co(en)_2Cl_2]Cl$ and $[Co(bipy)_3](NO_3)_2$ will be determined. The resulting catalysts will be characterized by Ultraviolet–visible spectroscopy (UV-VIS). Temperature-programmed reduction (TPR). Inductively coupled plasma mass spectrometry (ICP-MS). The investigation of catalytic performance on the effect of temperature, contact time, and selectivity towards products will be investigated by using the prepared single-site Co^{2+} on silica support.

1.2 Objectives

1.2.1 To prepare single-site Co^{2+} heterogeneous catalyst on silica supports using various cobalt complexes as a precursor

1.2.2 To study the cracking of cyclohexane using the prepared catalysts

1.2.3 To understand the mechanism of cyclohexane cracking over single-site heterogeneous catalysts

1.2.4 To understand the effect of temperature, contact time, carrier gas and prepared catalysts

1.2.5 To investigate the stability of the prepared catalysts

1.3 Scope of this study

1.3.1 Catalyst preparation by electrostatic adsorption methodology preparation single-site Co^{2+} heterogeneouson silica support using cobalt complexes and compared to the wetness impregnation of cobalt nitrate hexahydrate on silica support

1.3.2 Characterization of catalysts by Ultraviolet–visible spectroscopy (UV-Vis), Temperature-programmed reduction (TPR), and Inductively coupled plasma mass spectrometry (ICP-MS)

1.3.3 Testing on cyclohexane over various catalysts in a continuous fixed-bed reactor

1.3.4 Investigation on the effect of temperature (500, 550 and 600 °C), contact time (36, 72, and 144g.h/mol), carrier gas (N_2 and H_2), selectivity and ligand of cobalt complexes

1.3.5. Analysis and quantification of gas products by online gas chromatography with flame ionization detector (GC-FID)

1.4 Expected results

New technology for the production of cyclohexene from cyclohexane could be obtained. This technology could be an alternative methodology with the high selectivity of cyclohexene and less coke production. Furthermore, the knowledge of understanding cracking cyclohexane could be applied to other processes.

CHAPTER 2
LITERATURE REVIEWS AND THEORY

2.1 Catalysts

2.1.1 Types of catalysts

2.1.1.1 Homogeneous catalysts [14]

Typically homogeneous catalysts are dissolved in a solvent with the substrates. So, homogeneous catalysts act in same phase as the reactants. The mechanistic principles invoked in heterogeneous catalysts are generally applicable. One example of homogeneous catalysis involves the influence of H^+ on the esterification of methanoic acid and methanol forming methyl methanoate. For inorganic chiteria, homogeneous catalysis is often synonymous of organometallic catalysts. The advantages of homogeneous catalysts are high activity and excellent selectivity. While, the main disadvantages in this catalysts are difficulty to separate the catalysts; highly cost of catalysts recovery, and poor thermal stability.

2.1.1.2 Heterogeneous catalysts [14]

Heterogeneous catalysts act in different phase as the reactants. Most heterogeneous catalysts are solids that react with substrates in a liquid or gaseous reaction mixture. The diverse mechanisms for reactions on surfaces are known, depending on how the adsorption taking place. The dispersion of solid has the important effect on the reaction rate. If diffusion rates are not considered, the reaction rates for various reactions on surfaces depend merely on the rate constants and reactant concentrations. In addition, the total surface area of solid is critical since it determines the availability of catalytic sites. The smaller the catalyst particle size is the larger the surface area for a given mass of particle. The advantages of heterogeneous catalysts are easy and inexpensive of catalysts recovery and good thermal stability. Though, the main disadvantages in this catalyst is the selectivity, which is depending on multiple active sites.

2.2 Single-site heterogeneous catalysts

The single-site heterogeneous catalysts are classified as a type of heterogeneous catalysts. However it also behaves like homogeneous catalyst where the packet site of the active site can be governed by the environmentally surrounding on a support. The example of single-site heterogeneous catalyst is a monometallic linked to support by having tetrahedral structure. This catalyst has a discrete active site which is believed to be significant for their low coke formation and greater selectivity to the desired products than those observed over non-single-site heterogeneous catalysts of the similar composition.

The example of the single-site heterogeneous support on silica catalysts are single-site Zn^{2+} [13], single-site Co^{2+} [12], single-site Zr [15] and single-site Ta.[16] The preparation of single-site heterogeneous catalysts typically requires controlled synthetic techniques. Some of them needs to use the semi-stable compound as a reactant which requires the inert atmosphere environment. One interesting technique called electrostatic adsorption methodology is much more easier to handle. This method uses charge balance to bind a cation complex to a negatively charged silica surface in basic solution.

2.3 Cyclohexane

2.3.1 Cyclohexane production

Cyclohexane is a cycloalkane with the molecular formula C_6H_{12}. Cyclohexane has been produce as a by-product in the fractionation of natural gasoline. Alternatively, cyclohexane can be produced from hydrogenation of benzene.[1] In addition, cyclohexane is also produced by hydrogenation of toluene.

2.3.2 Cyclohexane application

Cyclohexane is primarily used as a chemical intermediate in the production of cyclohexanol and cyclohexanone, which are then used mainly to make adipic acid and caprolactam, respectively. Both of these are typically used to produce industrial materials, such as, nylon and other synthetic textiles. In addition, cyclohexane is also a chemical intermediate for the production of solvents and used to manufacture

benzene, an essential raw ingredient for the production of various plastics, dyes, epoxies, and certain pharmaceutical products.[17]

2.4 Cyclohexane cracking

2.4.1 Thermal cracking application [18]

Thermal cracking is a chemical process by which organic molecules are decomposed into lower molecular weight products. For example, the decomposition of cyclohexane in the presence of *n*-decane at 810 °C, cyclohexane has been is broken down into ethylene, hydrogen, 1,3-butadiene and small amount of cyclohexene as the reaction path is shown in **Figure 2.1**.

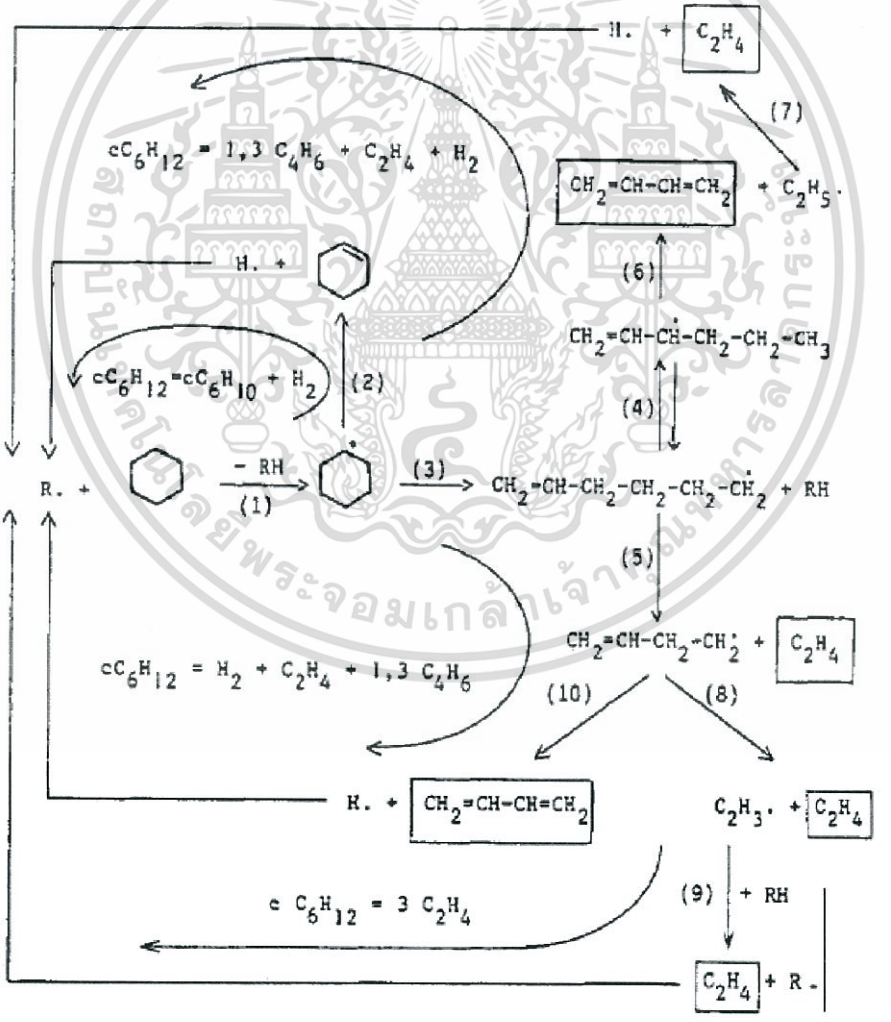

Figure 2.1 Reaction pathways of thermal cracking of cyclohexane

2.4.2 Catalytic cracking

Catalytic cracking is a chemical processes that use a catalyst in chemical reactions to reduce the activation energy resulting enhancement of reaction rate. The general catalysts are noble metal catalysts. Owing to the excellent activity, selectivity and stability, noble metals, such as, Platinum (Pt), Palladium (Pd), Ruthenium (Ru) and Rhodium (Rh) are used as catalysts in many heterogeneous catalytic reactions.[19] However, these noble metals are expensive. On the contrary, inexpensive metals that can activate C-H bond are Cobalt (Co), Ferrous (Fe) and Nickel (Ni).[11] Therefore, we are interested in single-site Co^{2+} heterogeneous catalysts prepared by using various cobalt complexes.

2.4.2.1 Oxidative dehydrogenation

Oxidative dehydrogenation is a chemical reaction that uses oxygen in reaction. It is an alternative routine to obtain cyclohexene as shown in **Equation 2.1**.

(Equation 2.1)

The catalysts in this reaction is metal oxide, such as, NiO [2], FeO_x [3] and Co_3O_4.[4] However, this routine exhibits low cyclohexene selectivity and produces significant amounts of CO_x. Thus, it is not favorable for industry point of view.

2.4.2.2 Dehydrogenation

Dehydrogenation is a chemical reaction using catalysts for the removal of hydrogen from a reactant shown in **Equation 2.2**. It is the reverse process of hydrogenation.

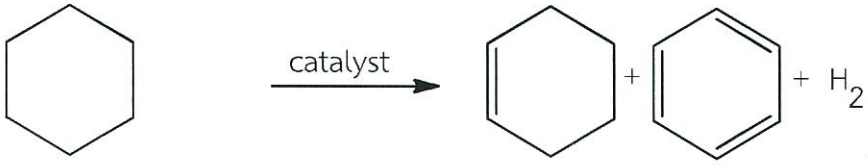

(Equation 2.2)

Pt/SiO_2 [5], Pt/Al_2O_3 [6], Ni/Al_2O_3 [9] and Ni/Al_2O_3-TiO_2[10] had been used for dehydrogenation of cyclohexane. Prior starting the reaction, the catalyst must be

reduced. Alternatively, single-site Co^{2+} heterogeneous catalysts can activate C-H and H–H bond. It had been also shown that the reaction occur via a non-redox mechanism as representing in **Figure 2.2**. The first step in this process is cyclohexane adsorption on the catalyst surface, the C-H bond in cyclohexane is heterolytically cleaved to form a cobalt alkylene (negative charge on the C) and bridging hydroxyl (proton from the C–H bond) group (intermediate 4). The resulting β-hydrogen transfer (5-TS) to form cyclohexene and a cobalt hydride in **Figure 2.2**. The resulting cobalt hydride then reacts with the neighboring hydroxyl proton to generate hydrogen, which desorbs to regenerate the initial Co–O resting state.

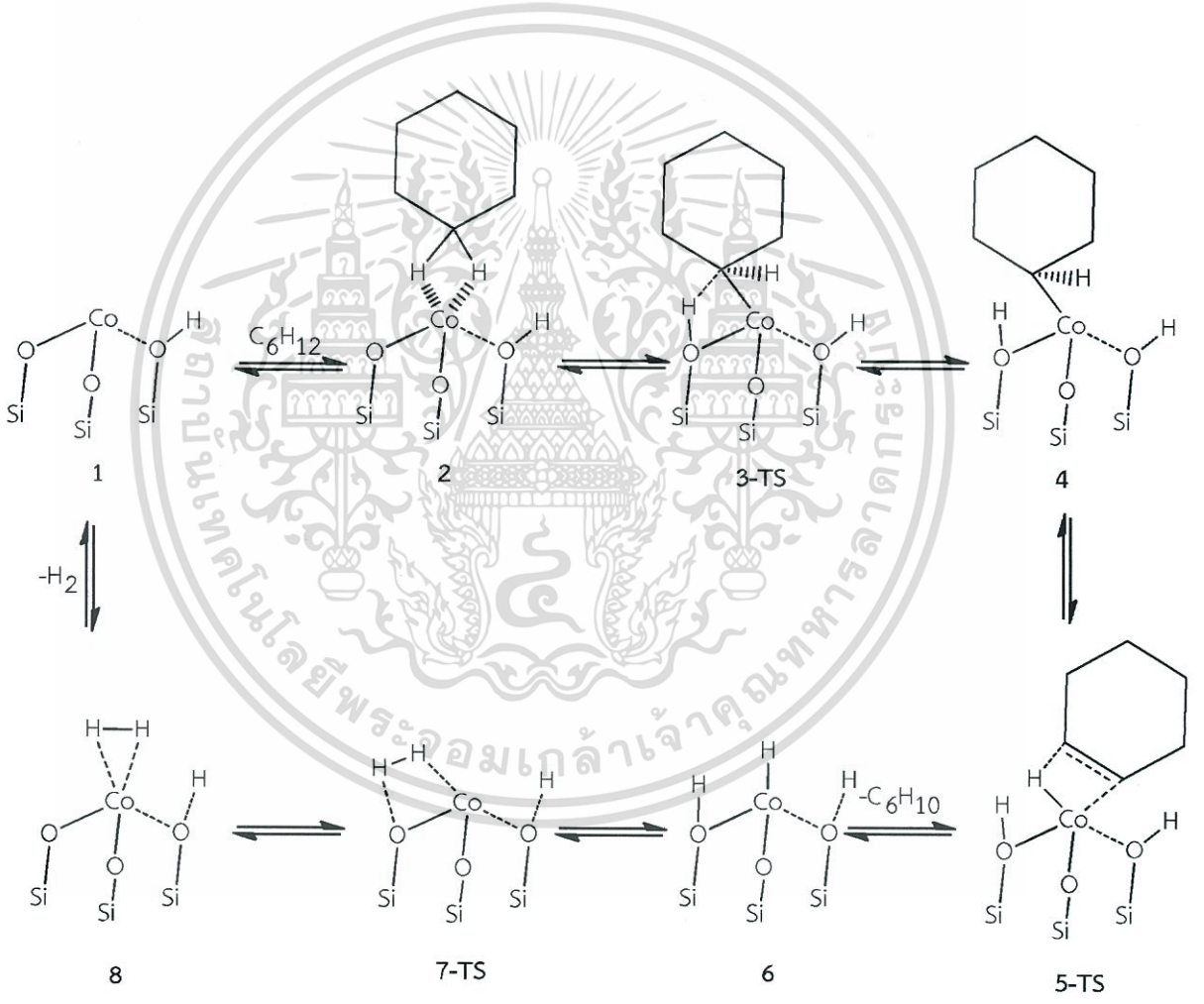

Figure 2.2 Catalytic reaction pathway for olefin hydrogenation and cyclohexane dehydrogenation on single-site Co^{2+} heterogeneous catalysts [13]

2.5 Literature reviews

The dehydrogenation of cyclohexane using various metals loaded on several supports has been investigated by Nai-liang and Seemeyer.[7,11]

Most of those catalysts generally produce coke during the reaction in which reduces the number of active sites and causes the deactivation of catalysts. In addition, the use of the noble metals is expensive.

Recently, the single-site Co^{2+} and Zn^{2+} heterogeneous catalysts had been reported that they can activate C-H and H–H bond by Schweitzer and Hu.[12,13]

These catalysts have a discrete active site which is believed to be significant for their low coke formation and greater selectivity to the desired products than those observed over non-single-site heterogeneous catalysts of the similar composition. Therefore, the single-site heterogeneous catalyst is of interest to be studied.

They studied about the effect of thermal cracking of cyclohexane in the presence of *n*-decane at approximately 810 °C by using the plug flow reactor. The result showed that cyclohexane chiefly decomposes into ethylene, hydrogen, 1,3-butadiene and small amounts of cyclohexene. Cyclohexane can undergo thermal cracking as shown by Billaud, F., et at., (1988).[18] The major drawbacks of this process are the use of high temperature and difficulty of product control.

The use of catalysts reduces the lower reaction temperature. AbdelDayem, H. M., et al., (2015), reported that the study of the effect of rare earth oxides doping of alumina support via oxidative dehydrogenation. The catalysts were prepared by impregnation of Nickel oxide on various type of alumina. The catalytic performance was investigated at 400°C. The result showed that the catalysts deactivated and produced significant amounts of CO_x.[2]

Nai-liang, W., et al., (2015), studied the effect of microwave calcination on catalytic properties of $Pt/MgAl(Sn)O_x$ catalyst in cyclohexane dehydrogenation to cyclohexene. The catalysts were prepared by impregnation method with hexachloroplatinic acid (H_2PtCl_6) as a reactant. The catalytic performance was studied at 550 °C. These catalysts showed well dispersion; however, during the reaction they show the high deactivation. These should be noted that the effect of microwave calcination altered strengthened the interaction between metal and support and facilitated the dispersion of the metal on support surfaces.[7]

Seemeyer, K., et al., (1995), reported the study of the face selectivity for the C-H bond activation of cyclohexane by first-row transition metal cations. The result showed that the late group 8 transition metal cations Fe^+, Co^+, and Ni^+ preferentially give a single cyclohexane dehydrogenation to form cyclohexene. Cr^+, Mn^+, and Zn^+ are unreactive toward cyclohexane, and the early transition metal cations Sc^+, Ti^+, and V^+ induce multiple dehydrogenation of cyclohexane to form benzene.[11]

Schweitzer, N.M., et al., (2014), studied about the selective dehydrogenation of propane to propylene. The catalyst is a single-site Zn^{2+} on heterogeneous catalysts silica support prepared via electrostatic adsorption methodology. The catalytic performance was studied at 550 and 650 °C. They found out that the single-site Zn^{2+} heterogeneous catalysts on silica support have highly selective dehydrogenation of propane to propylene (>95%).[13]

Hu, B., et al., (2015, reported the study of the propylene selectivity via dehydrogenation of propane over single-site Co^{2+} heterogeneous catalysts on silica support. The catalysts were prepared by two cobalt precursors, hexaamminecobalt(III) chloride ($[Co(NH_3)_6]Cl_3$) and cobalt(II) nitrate hexahydrate ($Co(NO_3)_2.6H_2O$), with the loadings of 0.125 or 5.00 g of cobalt precursors in 20 g of silica. The catalytic performance was investigated at 550 and 650 °C. The result showed that the single-site Co^{2+} heterogeneous catalysts on silica support has selectivities more than 95% at 550 °C and more than 90% at 650 °C with stable activity over 24 hours.[12]

CHAPTER 3

EXPERIMENTAL DETAILS

3.1 Chemicals and substrates

Table 3.1. Representing the chemical used in this study

Chemical reagents	Grade of purity	Manufacturers
1. Silicon dioxide (SiO_2)	99.00%	CARLO ERBA
2. Ammonia solution 30% (NH_4OH)	99.00%	CARLO ERBA
3. Ammonium chloride (NH_4Cl)	99.00%	CARLO ERBA
4. Cobalt(II) nitrate hexahydrate ($Co(NO_3)_2.6H_2O$)	98.00%	LABORATORY REAGENT (RANKEM)
5. Cobalt(II) chloride hexahydrate ($CoCl_2.6H_2O$)	99.00%	CARLO ERBA
6. 2,2'-bipyridine ($C_{10}H_8N_2$)	99.00%	SIGMA-ALDRICH
7. Ethylenediamine ($NH_2CH_2CH_2NH_2$)	99.00%	CARLO ERBA
8. Acetone ($(CH_3)_2CO$)	99.00%	FISHER SCIENTIFIC
9. Methanol (CH_3OH)	99.00%	FISHER SCIENTIFIC
10. 30% Hydrogen peroxide (H_2O_2)	99.00%	CARLO ERBA
11. Hydrochloric acid 37% (HCl)	99.00%	CARLO ERBA
12. Diethyl ether ($C_2H_5OC_2H_5$)	99.00%	CARLO ERBA
13. Cyclohexane (C_6H_{12})	99.00%	CARLO ERBA
14. Deionized water		
15. Activated charcoal		
16. Air zero gas, high purity	99.99%	PRAXAIR
17. Hydrogen gas, high purity	99.99%	PRAXAIR
18. Nitrogen gas, high purity	99.99%	PRAXAIR

3.2 Apparatus and instruments

1. Catalytic testing rig
2. Mass flow controller (BROOKS INSTRUMENT LLC)
3. Hot air Oven
4. Tube furnace with a programmed temperature controller (CARBOLITE)
5. Heating rod with a programmed temperature controller
6. Clamp
7. Gas chromatograph (Model 910, BUCK SCIENTIFIC)
8. Laboratory glass wares
9. Laboratory plastic wares
10. Trap condenser
11. Syringe (5 mL)
12. Syringe pump
13. Vial 13
14. Sieve (U.S.A standard sieve, AASHO N-92)
15. X-ray powder diffractometer (D8 Advance, Bruker AG)
16. Ultraviolet–visible spectroscopy (UV-VIS)
17. Fourier transform infrared spectroscopy (FTIR)
18. Inductively coupled plasma mass spectrometry (ICP-MS)
19. Temperature programmed reduction (TPR, Model TCD2-NIFED)
20. pH conductivity meter

3.3 Synthesis and preparation of catalysts

3.3.1 Synthesis of hexaamminecobalt(III) chloride, $[Co(NH_3)_6]Cl_3$

10.00 g of ammonium chloride (NH_4Cl) was dissolved in 40.00 mL of deionized water. With continuous stirring, 8.00 g of cobalt(II) chloride hexahydrate ($CoCl_2.6H_2O$) was added to the mixed gradually. Then, 40.00 mL of 15 M ammonium hydroxide (NH_4OH) was slowly added. The solution was stirred at ambient temperature for 30 seconds. After that, approximately 0.80 g of activated charcoal was introduced and added 17.00 mL of hydrogen peroxide (30% H_2O_2) while stirred all the time. When all bubbling has stopped, the reaction flask was placed in water bath at 60 °C for 40 minutes, and cooled with ice bath for the crystallization. The solids were filtrated by

vacuum filtration. Afterwards, all soilds were brought to 250 mL beaker with 100.00 mL of deionized water and 5.00 mL of 12 M HCl. When all orange solids was dissolved while heated, the activated charcoal was removed by the vacuum filtration. The remaining was added 15.00 mL of 12 M HCl, placed in ice bath for the crystallization for 2 hours. The orange crystals were filtrated by vacuum filtration. The products were collected and kept in non-moisture atmosphere.

3.3.2 Synthesis of pentaamminechlorocobalt(III) chloride, $[Co(NH_3)_5Cl]Cl_2$

1.70 g of ammonium chloride (NH_4Cl) was dissolved in 10.00 mL of 15 M ammonium hydroxide. With continuous stirring, 3.30 g of cobalt(II) chloride hexahydrate ($CoCl_2.6H_2O$) was added to the mixed gradually. When brown color slurry was obtained, 2.70 mL of 30% hydrogen peroxide was added slowly. After all bubbling has stopped, 10.00 mL of 12 M HCl was introduced slowly. With continued stirring, the mixture was heated on a hot plate and maintains 85 °C for 20 minutes, then the mixture was cooled to room temperature in an ice bath and filtrated by vacuum filtration. The crystals are washed with 5-6 times, 5.00 mL portions of cool water (deionized water cooled in ice) and then 5-6 times, 5.00 mL portions of ethanol.

3.3.3 Synthesis of *trans*-dichloro-*bis*-(ethylenediamine)cobalt(III) chloride, $[Co(en)_2Cl_2]Cl$

5.00 mmol of cobalt(II) chloride hexahydrate ($CoCl_2.6H_2O$) was dissolved in 9.50 mL of deionized water and added ethylenediamine ($NH_2CH_2CH_2NH_2$) solution (16%en in water 2.50 mL). The solution was drop-wise added by 30% H_2O_2 1.20 mL, then, evaporated at relative low temperature to approximately 2.00 mL of the solution, obtaining emerald green crystal. This crystal was washing with 16.00 mL of ethanol and 16.00 mL of diethyl ether, respectively.

3.3.4 Synthesis of *tris*-(bipyridine)cobalt(II) nitrate, $[Co(bipy)_3](NO_3)_2$

3.00 mmol of cobalt(II) nitrate hexahydrate ($Co(NO_3)_2.6H_2O$) and 11.00 mmol of 2,2'-bipyridine ($C_{10}H_8N_2$) were dissolved in a minimum volume of methanol. The solution was stirred at ambient temperature for 2 hours and left for 24 hours for precipitation. The yellowish crystals were collected and kept in a desiccator.

3.3.5 Preparation of catalysts

3.3.5.1 Silica support (SiO_2)

Silica was calcined in muffle oven by ramping to 600 °C at the heating rate of 5°C/minutes and holding for 1 hour.

3.3.5.2 Preparation of single-site Co^{2+} heterogeneous catalysts on silica support ($CoII/SiO_2$)

10.00 g of silica were suspended in approximately 100.00 mL of deionized water. The pH of the solution was adjusted to 11 using concentrated ammonium hydroxide (NH_4OH). In a separate flask, 2.50 g of cobalt complex (The cobalt complex precursors are shown in **Table 1.1.**) was dissolved in 25.00 mL of deionized water. The pH of the solution was adjusted to 11 with NH_4OH. The cobalt solution was rapidly added to the silica and stirred for 10 minutes at room temperature. The solid was allowed to settle for 5 minutes. The resulting wet powder was vacuum filtered, rinsed several times with deionized water, and dried at room temperature for 8 hours, followed by drying in air at 125 °C for 8 hours. Afterward, the catalyst was calcined in muffle oven by ramping to 600 °C at the heating rate of 5°C /min and holding for 1 hour.

Table 3.2. The cobalt complex precursors used in catalyst's preparation

Cobalt complexes	Formula
hexaamminecobalt(III) chloride	$[Co(NH_3)_6]Cl_3$
pentaamminechlorocobalt(III) chloride	$[Co(NH_3)_5Cl]Cl_2$
trans-dichloro-*bis*-(ethylenediamine)cobalt(III) chloride	$[Co(en)_2Cl_2]Cl$
tris-(bipyridine)cobalt(II) nitrate	$[Co(bipy)_3](NO_3)_2$

3.3.5.3 Preparation of 5%wt cobalt on silica catalysts (Co/SiO_2)

The 5%wt cobalt on silica support was prepared by wet impregnation method. In the first step, 2.5991 g. of cobalt nitrate hexahydrate ($Co(NO_3)_2.6H_2O$) was dissolved in deionized water 20.00 mL. After that, 10.00 g of SiO_2 was impregnated by the solution. The solid was dried in oven at 125 °C for 8 hours. Then, the dried catalyst

was calcined in muffle oven by ramping to 600 °C for 1 hour with a heating rate 5 °C/min.

3.4 Cobalt complexes and catalyst characterization

3.4.1 Fourier transform infrared spectroscopy (FT-IR)

The cobalt complexes structure was determined to find the functional group. The powder of the sample was pressed about 5 tons into a disc. Infrared spectra were collected using Spectrum GX (Perkin Elmer) at Scientific Instrument Service Centre, KMITL, from 400-4000 cm^{-1}. The IR signal was calibrated and corrected employing polystyrene film as a standard.

3.4.2 Ultraviolet–visible spectroscopy (UV-VIS)

Ultraviolet–visible spectroscopy (UV-VIS) was used to determine the Co loading amount, using deionized water is adjusted pH 11 was used as solvent for baseline correction. The sample solution is taken to adjust the volume to a certain volume. The calibration curve was prepared with a sample standard in different concentrations. The samples were measured using a UV–Vis Spectrophotometer (PG instruments limited, T60 U, 50-60 Hz, 150 W), with a wavelength of maximum absorbance. The results were calculated for finding the Co loading amount.

3.4.3 Temperature-programmed reduction (TPR)

Temperature-programmed reduction (TPR) provides information on the active site species of the catalysts by monitoring their reducibility and determine the %Co loading of the catalysts. Temperature programmed reduction was measured using thermal conductivity detector (TCD). The sample weighed 100 mg was placed into a quartz tube reactor, which was located inside a temperature-regulated furnace. Prior to the H_2-TPR, each sample was heated to its activations temperature in air zero (30 mL/min) for 1 hours with 5 °C /min and was cooled down to below 40 °C. The heating rate of 10 °C/min, 20 mL/min of 10% H_2 in Ar was applied for TPR analysis. Water production during the reduction process was removed in a U-shape tube trap before entering the TCD.

3.4.4 Inductively Coupled Plasma Mass Spectrometry (ICP-MS)

Inductively coupled plasma mass spectrometry (ICP-MS) was used to determine the Co loading amount. ICP-MS was performed on a Thermo Scientific iCAP Qc ICP-MS. Sample solvents were evaporated and the organic components were removed by heating at 625 °C for several hours and analyzed by ICP-MS. The flow rate on the instrument was 1 mL/min and dual detector mode was employed. A blank was subtracted after internal standard correction and the value reported are an average of three reading.

3.5 Catalytic testing

Gas phase catalytic conversion of cyclohexane was investigated at atmospheric pressure in a continuous fixed-bed reactor made with glass tube (8.0 mm O.D.). Schematic of the catalytic testing rig is shown in **Figure 3.1**. The catalyst bed was packed in the middle of the reactor and topped with quartz wool and quartz beads. The reactor was then installed inside a temperature-controlled electrical furnace. The gas flows were controlled by the mass flow controllers and checked by bubble flow meter. Before the testing, the catalyst was activated by heating at 5 °C /min to its calcinations temperature (600 °C) and was hold at that temperature for 1 hour under the stream of N_2 (30 mL/min). Finally, the reaction was run at 550 °C (450-600 °C) hold 6 hours.

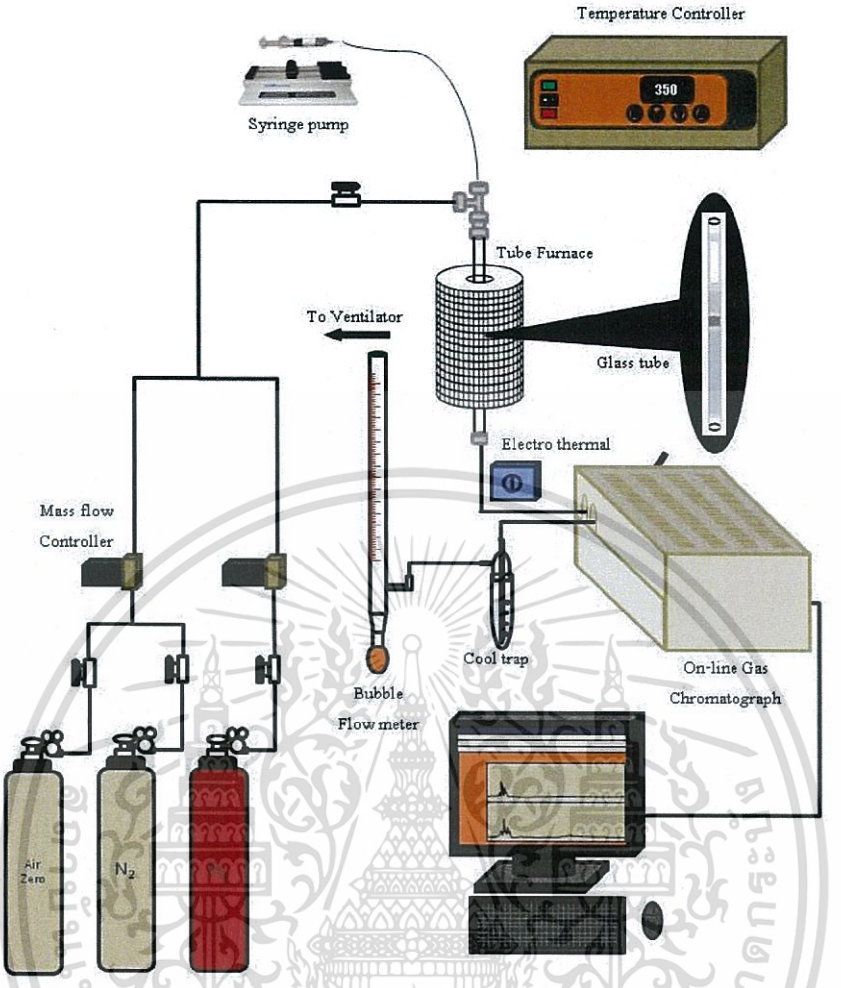

Figure 3.1 Schematic of the catalytic testing rig

In each run, cyclohexane was passed through the catalyst bed under a 60 mL/min flow of N_2. The catalytic testing was continued for at least 6 hours on stream. The reacted gaseous mixture was flowed out of the reactor and passed through a gas sampling loop. In order to prevent condensation of products, the line after reactor was heated by heating rods. Description of the reactor set up and the reaction conditions are summarized in **Table 3.3.**

Table 3.3 Description of the reactor set up and reaction condition

Parameters	Value
Reactor outside diameter (mm)	8
Bed length (mm)	12-72
Total flow (mL/min)	60
Catalyst weight (g)	0.2-1.0
Contact time (g.h/mol)	36-144
Catalyst activation (before reaction)	Heating rate: 5 °C/min Calcination temperature: 600 °C Gas: N_2 (30 mL/min)
Reaction temperature	450-600 °C
Reaction total pressure	Atmospheric pressure (1 atm)

3.6 Analysis products

The product analysis was generally performed using an online gas chromatograph. The gas sample was collected in gas sampling loop, then periodically injected into GC column (HP-5, 30 m length, 0.32 mm internal diameter, 0.25 μm film thickness) connected to flame ionized detectors (FID). The following temperature program was used for the analysis: holding at 35 °C for 9 min., followed by the ramping to 100 °C at the rate of 15 °C/min. holding 30 sec., then ramping to 220°C at the rate of 15 °C/min. N_2 gas was used as a carrier gas. Each component was separated as they pass though the column with an inert carrier N_2 gas and their presence in the effluent were recorded as a chromatogram. Each peak areas from the chromatogram was measured and calculated. Then each peak was identified by comparing with standard and the composition of each product was determined by calibration of standard.

CHAPTER 4

RESULTS AND DISCUSSION

4.1 Cobalt complexes characterization

The characterization of cobalt complexes provides the information indicating the complex formation and composition. Hexaamminecobalt(III)chloride ($[Co(NH_3)_6]Cl_3$), *trans*-dichloro-*bis*-(ethylenediamine)cobalt(III)chloride($[Co(en)_2Cl_2]Cl$), pentaamminechlorocobalt(III)chloride($[Co(NH_3)_5Cl]Cl_2$) and *tris*-(bipyridine)cobalt(II) nitrate ($[Co(bipy)_3](NO_3)_2$) used as a precursor, were initially characterized by the following method: Fourier Transform Infrared Spectroscopy (FTIR) and Ultraviolet-Visible Spectroscopy (UV-Vis).

4.1.1 Fourier transform infrared spectroscopy (FTIR)

The FTIR spectra of $[Co(NH_3)_6]Cl_3$, $[Co(NH_3)_5Cl]Cl_2$, $[Co(en)_2Cl_2]Cl$ and $[Co(bipy)_3](NO_3)_2$ are shown in **Figure 4.1**.

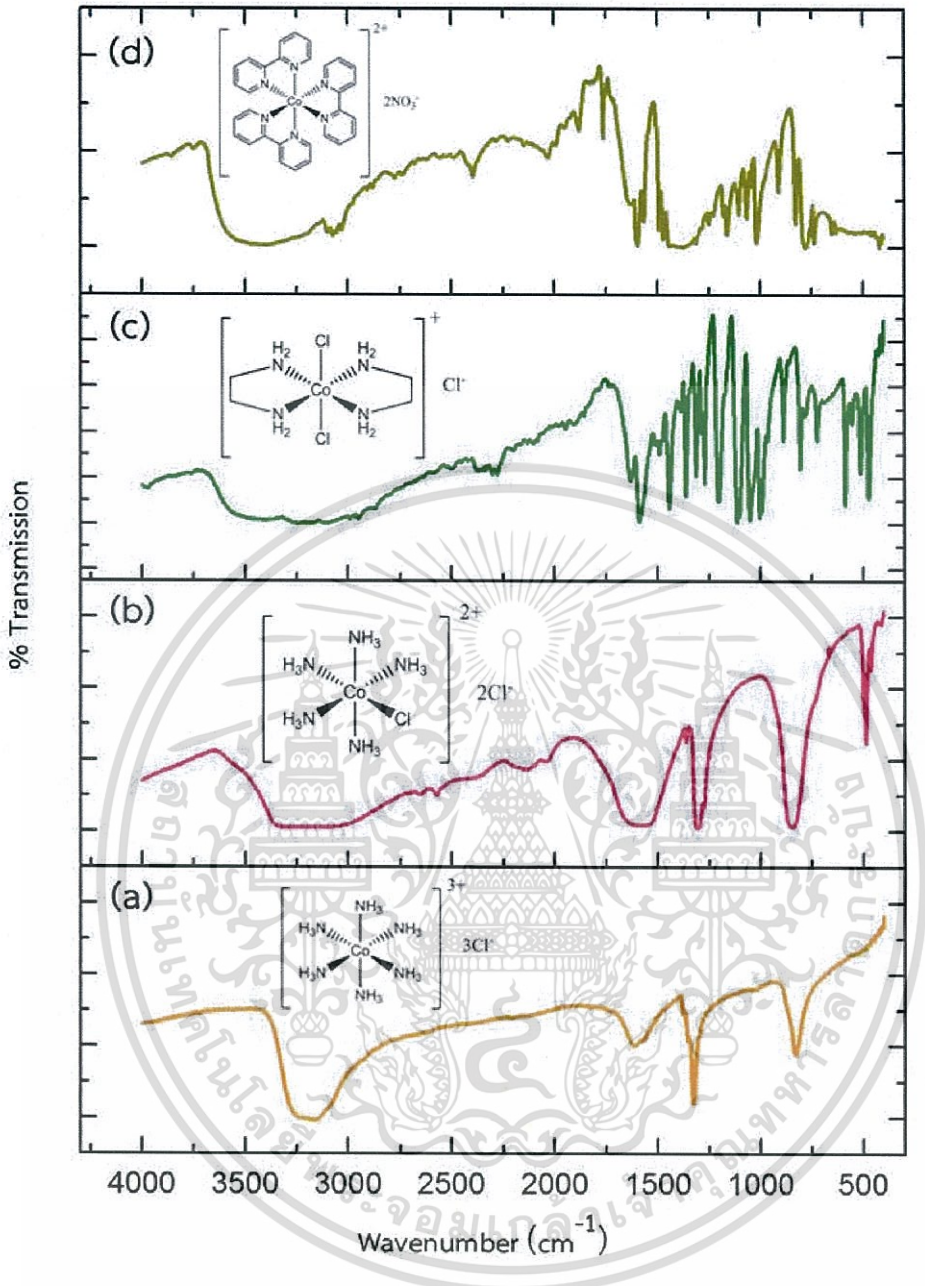

Figure 4.1 FTIR spectra of $[Co(NH_3)_6]Cl_3$ (a), $[Co(NH_3)_5Cl]Cl_2$ (b), $[Co(en)_2Cl_2]Cl$ (c) and $[Co(bipy)_3](NO_3)_2$ (d)

The spectra of $[Co(NH_3)_6]Cl_3$ (**Figure 4.1a**) shows the peak at 3250 cm^{-1}, ascribed to N-H stretching from coordinated ammonia ligand. The peaks at 1602, 1363, 824 cm^{-1} belong to N-H bending.[20]

The spectra of $[Co(NH_3)_5Cl]Cl_2$ (**Figure 4.1b**) shows the broad band from 3715 to 3320 cm^{-1}, assigned to vibrational stretching mode of O-H due to adsorbed atmospheric water. The peak at 3283 cm^{-1}, ascribed to N-H stretching from coordinated ammonia ligand. The peak at 1595, 1362, 844 cm^{-1} belong to N-H bending. The vibration bands of Co-N is at 488 cm^{-1}.[20]

The spectra of $[Co(en)_2Cl_2]Cl$ (**Figure 4.1c**) shows the broad band from 3715 to 3320 cm^{-1}, assigned to vibrational stretching mode of O-H due to adsorbed atmospheric water. The peaks at 3217 cm^{-1} and 2943 cm^{-1} are ascribed to N-H stretching and C-H stretching from coordinated ethylenediamine ligand, respectively. The peaks at 1573, 1446, 1200 to 1040 and 480 cm^{-1} belong to N-H bending, C-N bending, C-N stretching and Co-N, respectively.[21]

The spectra of $[Co(bipy)_3](NO_3)_2$ (**Figure 4.1d**) shows the broad band from 3715 to 3300 cm^{-1}, assigned to vibrational stretching mode of O-H due to adsorbed atmospheric water. The intense peak at 3030 cm^{-1} is ascribed to C-H stretching from coordinated bipyridine ligand. Multiple peaks around 1940 cm^{-1} are overtones of aromatic and the intense peak at 1580 and 1558 cm^{-1} belong to C=N stretching. The vibration bands of C-N stretching, C-H bending and C-N bending are at 1416 cm^{-1}, 1300 to 900 cm^{-1} and 757 cm^{-1}, respectively.[22]

4.1.2 Ultraviolet-visible spectroscopy (UV-Vis)

The UV-Vis absorption spectra of all complexes in water solution at pH 11 scanning from 300 to 600 nm are shown in **Figure 4.2**.

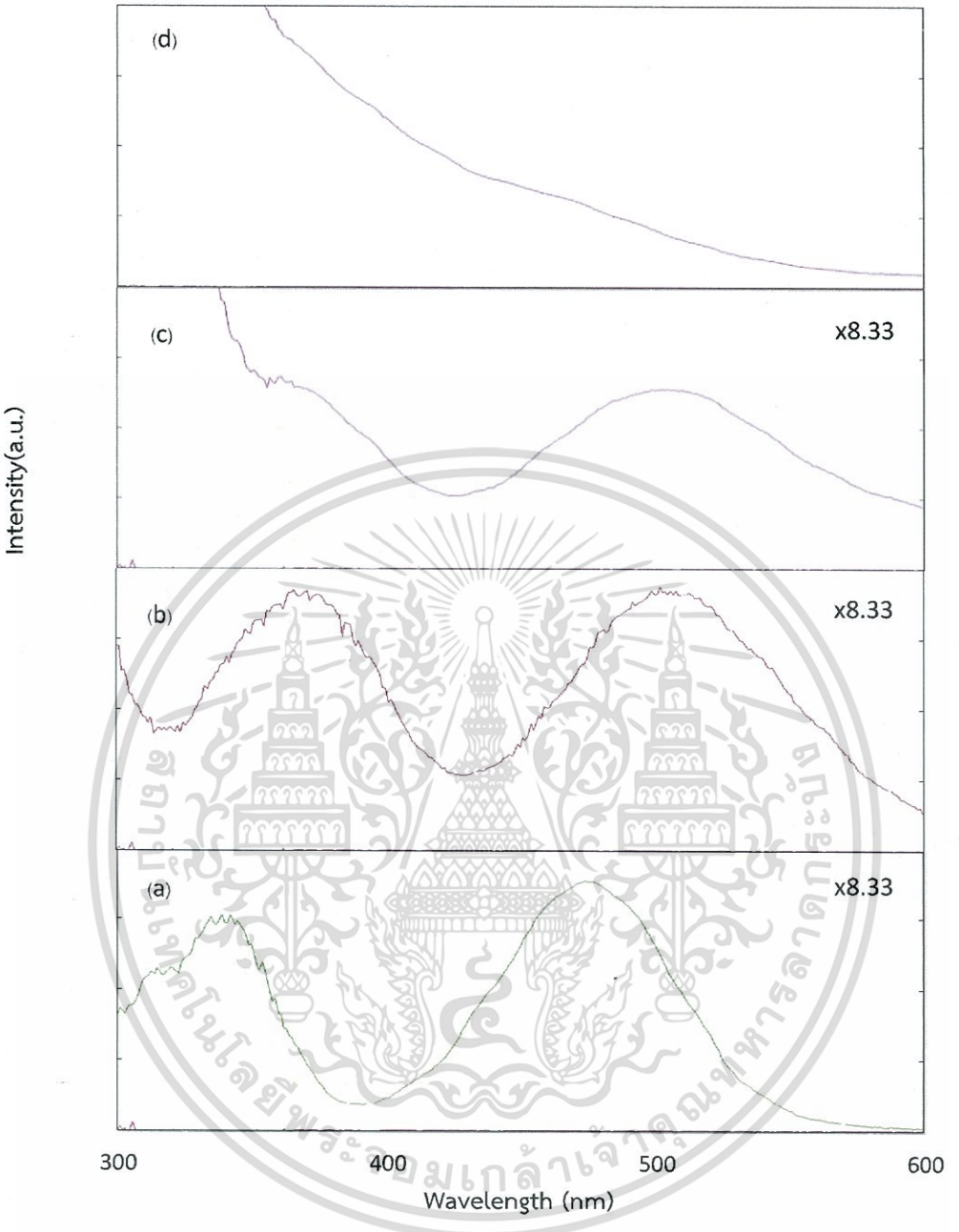

Figure 4.2 UV-Vis spectra of $[Co(NH_3)_6]Cl_3$(a), $[Co(NH_3)_5Cl]Cl_2$(b), $[Co(en)_2Cl_2]Cl$(c) and $[Co(bipy)_3](NO_3)_2$(d)

The absorption peak of all complexes is shifted, which due to the electronic effect induced by the coordinated ligands. $[Co(NH_3)_6]Cl_3$ absorbance appears at 475 nm, corresponding to a yellow-orange crystalline; whereas, $[Co(NH_3)_5Cl]Cl_2$, pink crystalline, is positioned at 502 nm. *trans*-$[Co(en)_2Cl_2]Cl$ normally shows the absorbance at 615 nm. However, in the basic solution, isomerization of *trans*- to *cis*-

takes place crossing the isomer changestruly the pink. Therefore, *cis*-$[Co(en)_2Cl_2]Cl$ absorbance appears at 505 nm. $[Co(bipy)_3](NO_3)_2$ shows the absorption at 438 nm in consistent, to the yellow crystalline.

All absorption peaks of all complexes are similar to those previously reported. [23-26]

4.2 Catalyst characterization

4.2.1 Adsorption of cobalt complexes on silica support

Each cobalt complex ($[Co(NH_3)_6]Cl_3$, $[Co(NH_3)_5Cl]Cl_2$, $[Co(en)_2Cl_2]Cl$, and $[Co(bipy)_3](NO_3)_2$) was loaded on SiO_2 which was calcined at 600 °C prior to adsorption (section 3.3.5.1). The determination of %Co loading on silica was investigated by using Ultraviolet–Visible Spectroscopy. The calibration curve of each Cobalt complexes are shown in the Appendix A. In summary, the amounts of adsorbed cobalt on calcined silica are shown in **Table 4.1**.

Table 4.1 The amounts of adsorbed cobalt and Co that loaded on SiO_2

	Cobalt solution (mmol)	Remain Cobalt solution (mmol)	Adsorbed Cobalt (mmol)	%Co (mmol/g.cat)	% Co (%wt)
$[Co(NH_3)_6]Cl_3$	4.3867	3.1584	1.2283	24.22	1.43
$[Co(NH_3)_5Cl]Cl_2$	4.6480	3.9055	0.7425	14.72	0.87
$[Co(en)_2Cl_2]Cl$	5.0176	-	-	-	-
$[Co(bipy)_3](NO_3)_2$	6.0940	5.9021	0.1919	3.82	0.23

Note: The absorption of $[Co(en)_2Cl_2]Cl$ could not determine by UV-Vis technique due to the red shifted peaks.

From the UV-Vis spectroscopy, the adsorption ability of cobalt complexes follows $[Co(NH_3)_6]Cl_3$ > $[Co(NH_3)_5Cl]Cl_2$ > $[Co(bipy)_3](NO_3)_2$. The adsorption of $[Co(NH_3)_6]Cl_3$ complex on silica is higher than other complexes because it possesses high charge density. Therefore, it could interact with the negative charge on the silica

surface. The charge density of complexes is in the order of $[Co(NH_3)_6]Cl_3$ > $[Co(NH_3)_5Cl]Cl_2$ > $[Co(en)_2Cl_2]Cl$ > $[Co(bipy)_3](NO_3)_2$. Hence, the adsorption ability of the cobalt complexes on silica surface depends on the charge density.

Due to the shifts of λ_{max} of the remaining solution, loading of $[Co(en)_2Cl_2]Cl$ cannot be analyzed by using UV-Vis spectroscopy. In order to find the Cobalt adsorbed on silica, H_2-Temperature programmed reduction (H_2-TPR) and Inductively coupled plasma mass spectrometry (ICP-MS) were used as the alternative technique.

4.2.2 Temperature programmed reduction (TPR)

Temperature programmed reduction profiles of non-single-site Co heterogeneous and single-site Co^{2+} heterogeneous on SiO_2 catalysts were investigated by H_2-temperature programmed reduction (H_2-TPR). The H_2-TPR profiles of non-single-site Co heterogeneous catalyst prepared by the wetness impregnation and single-site Co^{2+} heterogeneous catalysts prepared by electrostatic adsorption methodology are shown in **Figure 4.3**.

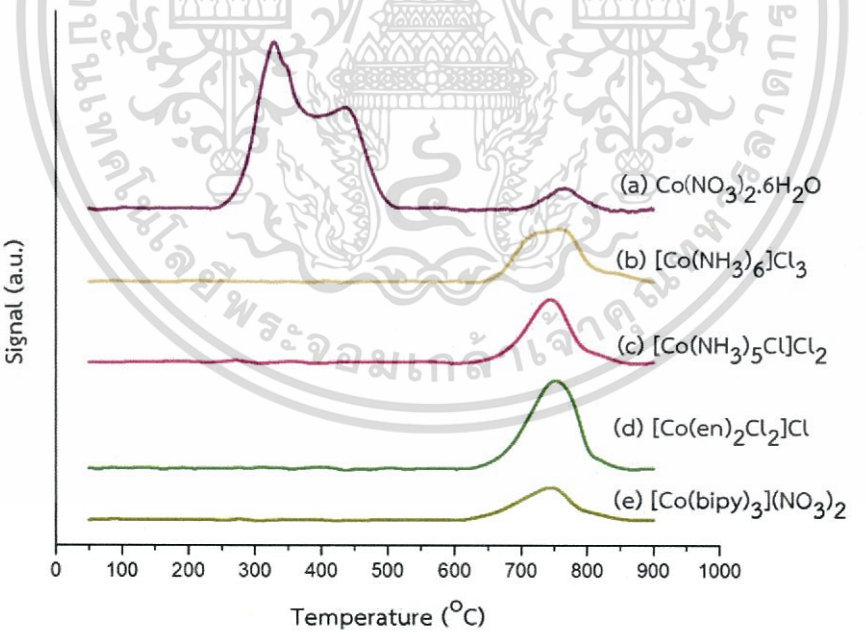

Figure 4.3 TPR profile of non-single-site Co and single-site Co^{2+} on SiO_2 prepared by using various precursor: $Co(NO_3)_2.6H_2O$ (a); $[Co(NH_3)_6]Cl_3$ (b), $[Co(NH_3)_5Cl]Cl_2$ (c), $[Co(en)_2Cl_2]Cl$ (d), $[Co(bipy)_3](NO_3)_2$ (e) (10% H_2/Ar, ramping at 10 °C/min)

As seen from **Figure 4.3a,** two main reduction peaks at 330 °C and 440 °C are observed for non-single-site Co/SiO_2 catalyst prepared with $Co(NO_3)_2.6H_2O$ precursor. The first peak is assigned to the reduction of Co_3O_4 to CoO, and the other is the subsequent reduction of CoO to metallic Co.[27] Moreover, the reduction peak around 700-850°C is observed with red extent, indicating the reduction of isolated Co^{2+}, presumably as cobalt silicate. In the case of single-site Co^{2+}/SiO_2 catalyst, the peak at 650-850 °C represents the reduction of Co^{2+} to metallic Co.

The loading of Co on SiO_2, corresponded to the hydrogen consumed, can be calculated from the peak area of the H_2-TPR profile. The peak of hydrogen consumption for reduction CuO standard was compared. In order to confirm loading of Co on SiO_2 of each catalyst, the ICP-MS of all catalysts was investigated. The results are shown in **Table 4.2**.

Table 4.2 Amounts of Co that loaded on SiO_2

Precursor	TPR			ICP-MS
	%Cobalt species (%wt)		%Co	%Co
	non-single-site	single-site	(%wt)	(%wt)
$[Co(NH_3)_6]Cl_3$	-	1.14	1.14	1.64
$[Co(NH_3)_5Cl]Cl_2$	-	0.93	0.93	1.40
$[Co(en)_2Cl_2]Cl$	-	1.53	1.53	2.01
$[Co(bipy)_3](NO_3)_2$	-	0.63	0.63	0.84
$Co(NO_3)_2.6H_2O$	4.09	0.71	4.80	4.85

As seen from **Table 4.2**, the impregnation method gives highest cobalt loading as non-single-site species (4.09%) and single-site species (0.71%). For the single-site catalysts, cobalt loading (by adsorption technique) is increased in the order of from $[Co(bipy)_3](NO_3)_2$ (0.63%) < $[Co(NH_3)_5Cl]Cl_2$ (0.93%) < $[Co(NH_3)_6]Cl_3$ (1.14%) < $[Co(en)_2Cl_2]Cl$ (1.53%). This trend is in line to the result from the UV-Vis adsorption (section 4.2.1). However, *tran*-$[Co(en)_2Cl_2]Cl$ is an exception because, in the basic solution, isomerization of *trans*-$[Co(en)_2Cl_2]^{1+}$ ion to *cis*-$[Co(en)_2Cl_2]^{1+}$ ion take place. The *cis*-$[Co(en)_2Cl_2]^{1+}$ ion having 2 monodentate and 2 bidentate ligands, could have a better geometry to interact with the negative charge on the silica surface, as compared to other cobalt complexes.

The ICP-MS results, give a trend of cobalt loading similar to TPR technique.

4.3 Catalytic testing

4.3.1. Effect of carrier gas flow rate

The effect of carrier gas flow rate towards cyclohexane conversion over Co^{2+}/SiO_2 ($[Co(NH_3)_6]Cl_3$ as a precursor) were investigated by using nitrogen as a carrier gas. The conversion of cyclohexane at various gas flow rate (50-80 mL/min) is shown in **Figure 4.4**.

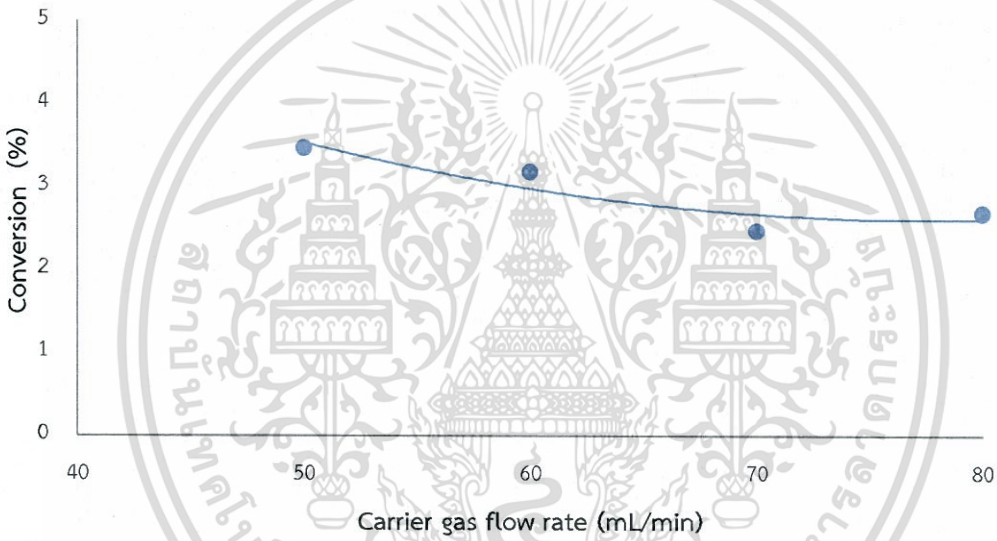

Figure 4.4 Conversion of cyclohexane at various N_2 flow rate
(Reaction condition; Temperature: 550 °C, Pressure: 1 atm, Contact time: 36 g.h/mol, Flow rate of N_2 carrier gas 50-80 mL/min, Average results at 160 minutes of time on stream)

The conversion of cyclohexane is slightly decreased as the gas flow rate is increased particularly at flow rate higher than 60 mL/min. This could be due to the through packed bed diffusion at high flow rate. Therefore, the flow rate of 60 mL/min was used for the investigation.

4.3.2. Effect of Contact time

In order to study the reaction mechanism, the effect of contact time towards cyclohexane conversion over Co^{2+}/SiO_2 ($[Co(NH_3)_6]Cl_3$ as a precursor) were investigated. The conversion of cyclohexane at various contact time (36-144 g.h/mol) is represented in **Figure 4.5**.

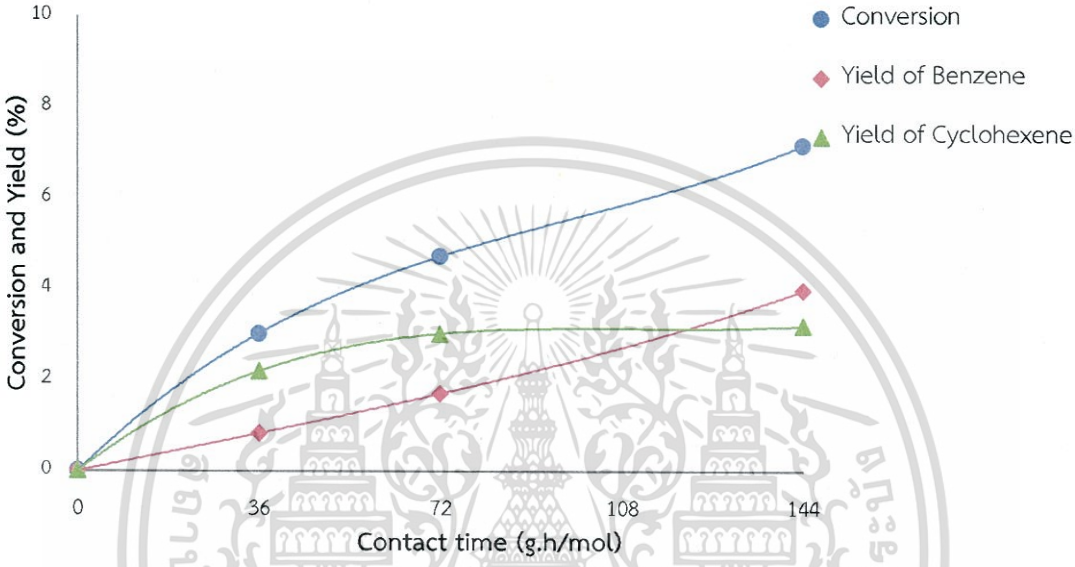

Figure 4.5 Conversion of cyclohexane and yield of products at various contact times by weight variation of catalyst (Reaction condition; Temperature: 550 °C, Pressure: 1 atm, Contact time: 36-144 g.h/mol, Flow rate of N_2 carrier gas 60 mL/min, Average results at 200 minutes of time on stream)

Upon increasing the contact time, the conversion of cyclohexane is rising from 3.0% (36 g.h/mol), 4.7% (72 g.h/mol) to 7.2% (144 g.h/mol). This is because that the higher the contact time, the higher the amount of catalyst. Hence, cyclohexane has a higher chance to interact with the active sites.

Considering the products yield, it is observed that increasing the contact time, cyclohexene yield is slightly increased to a certain level (3.2%). The benzene yield is increased gradually. This is suggested that cyclohexene can be converted to benzene in a series reaction pathway. However, at low contact time, the benzene can also be obtained. It is suggested that there is also a chance for cyclohexane to convert directly to benzene. In other words, benzene are generated in parallel. The reaction pathway can be proposed has shown in **Scheme 4.1**.[28]

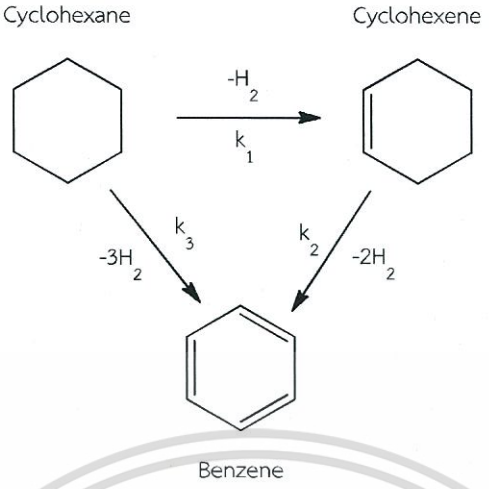

Scheme 4.1 Dehydrogenation of cyclohexane

The selectivity to products at various contact times is represented in **Figure 4.6**.

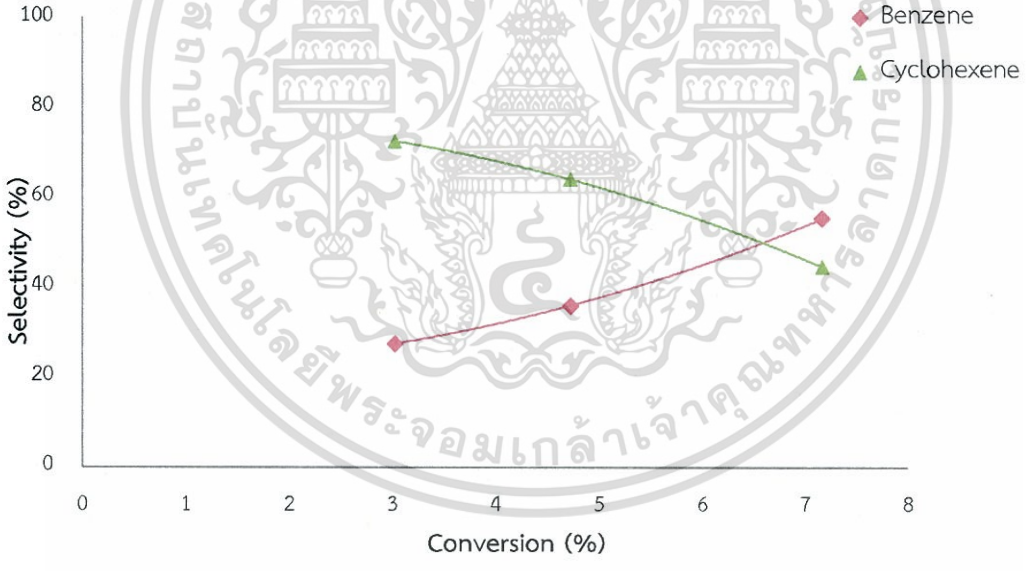

Figure 4.6 Selectivity towards each products at various contact times by weight variation of catalyst

In a support manner with the above discussion, **Figure 4.6** shows that the selectivity of benzene is increased. While, the selectivity of cyclohexene is decreased with contact time.

Since cyclohexene is designed products for the precursor in the production of caprolactam and cyclohexanol. At contact time of 36 g.h/mol, high selectivity of cyclohexene is obtained. Therefore, the contact time of 36 g.h/mol is chosen for further study.

4.3.3. Effect of reaction temperature

The effect of reaction temperature towards cyclohexane conversion over Co^{2+}/SiO_2 ($[Co(NH_3)_6]Cl_3$ as a precursor) were studied. The cyclohexane conversion and yield of products at various reaction temperatures (450-600 °C) are shown in **Figure 4.7**.

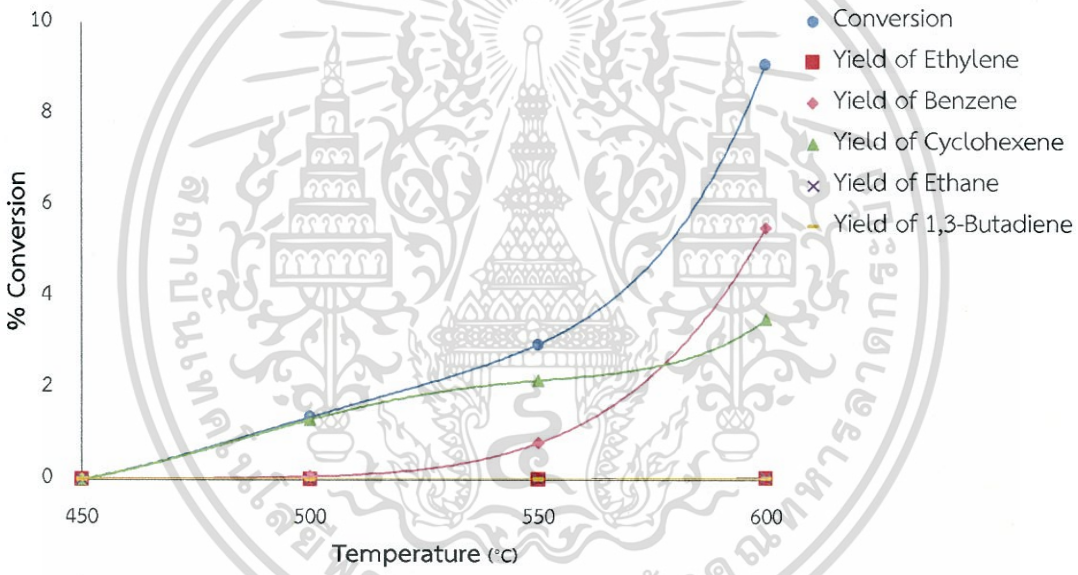

Figure 4.7 Conversion of cyclohexane and yield of products at various reaction temperatures (Reaction condition; Temperature: 450-600 °C, Pressure: 1 atm, Contact time: 36 g.h/mol, Flow rate of N_2 carrier gas 60 mL/min, Average results at 360 minutes of time on stream)

The results show that as the temperature is increased, the conversion is increased from 0% (450 °C), 1.4% (500 °C), 3.0% (550 °C) to 9.1% (600 °C). It is suggested that increasing the temperature, the rate of a reaction is also increased. At all temperatures the main products from this reaction are cyclohexene and benzene. However, at 600 °C the ethylene, ethane and 1,3-butadiene were observed from the

cracking of cyclohexane or cyclohexene. The selectivity towards each product at various reaction temperatures is summarized in **Table 4.3**.

Table 4.3 Selectivity towards each product at various reaction temperatures

Temperature (°C)	Conversion (%)	Selectivity of products (%)				
		Ethylene	Ethane	1,3-Butadiene	Cyclohexene	Benzene
450	0	-	-	-	-	-
500	1.4	-	-	-	95.7	4.3
550	3.0	-	-	-	73.2	26.8
600	9.1	0.2	0.4	0.2	39.1	60.1

As seen from **Table 4.3**, increasing the temperature, the selectivity of benzene keeps enhancing. On the other hand, the selectivity of cyclohexene is decreased. This can be explained that increasing the temperature affects the cracking of cyclohexene to benzene (k_2) and the cracking of cyclohexane to benzene (k_3). As the temperature is increased the value of k_2 and k_3 would also be increased.

In the mechanistic point of view, ethylene, ethane and 1,3-butadiene could be derived from thermal cracking of cyclohexene or cyclohexane at high temperature (>550 °C).[18] However, they could also be produced from the catalytic cracking over single-site Co^{2+}/SiO_2. Furthermore, ethylene could be hydrogenated to ethane (The Gibbs free energy are shown in Appendix E). The overall reaction pathways for cyclohexane conversion over single-site Co^{2+} can be proposed as shown in **Scheme 4.3.**

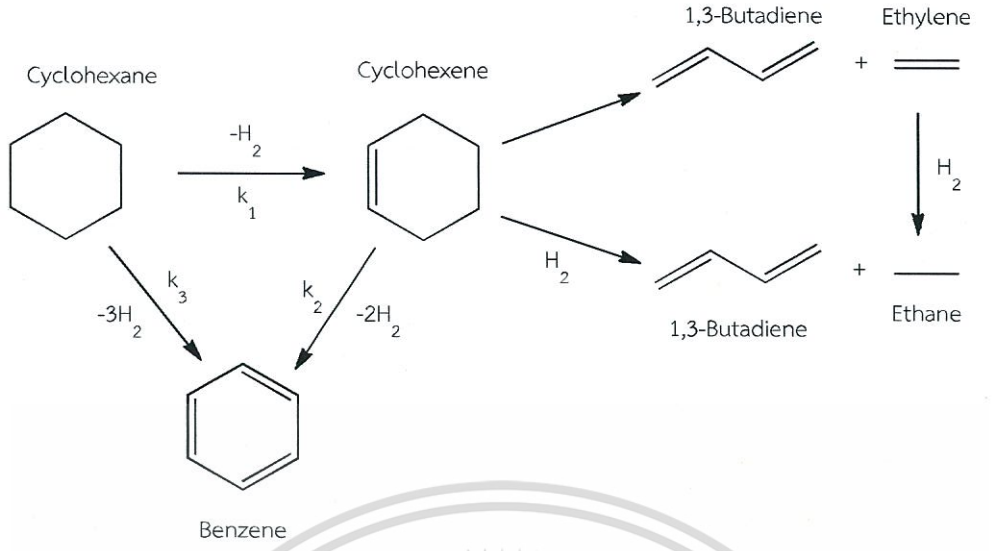

Scheme 4.3 Overall mechanism of the conversion of cyclohexane over single-site Co^{2+}/SiO_2

At temperature 550 °C shows higher the selectivity of cyclohexene. Therefore, this temperature is chosen for further study.

4.3.4. Effect of carrier gas

In order to study the effect of carrier gas, using hydrogen or nitrogen as a carrier gas were studied for cyclohexane conversion over Co^{2+}/SiO_2 ($[Co(NH_3)_6]Cl_3$ as a precursor). The cyclohexane conversion and selectivity towards each product under N_2 or H_2 atmosphere are shown in **Table 4.4**.

Table 4.4 Conversion of cyclohexane and selectivity towards each product under N_2 and H_2 atmosphere

Carrier gas	Conversion (%)	Selectivity of products (%)			
		Ethylene	Ethane	Cyclohexene	Benzene
N_2	3.0	-	-	73.21	26.79
H_2	9.1	10.38	0.02	15.17	74.43

(Reaction condition; Temperature: 550 °C, Pressure: 1 atm, Contact time: 36 g.h/mol, Flow rate of carrier gas 60 mL/min, Average results at 360 minutes of time on stream)

As seen from **Table 4.4**, the conversion of cyclohexane using H_2 as a carrier gas is higher than that using N_2 as a carrier gas. This can be explained that the interaction of hydrogen with single-site cobalt could lead to the formation of cobalt hydride that possesses higher activity, as compared to single-site cobalt.

For the product selectivity, these changes in selectivity of benzene may be derived from the change in conversion.

For ethylene and ethane, they could also be produced from the catalytic cracking over cobalt hydride species.

As the selectivity of cyclohexene is higher for the reaction using N_2 gas, N_2 was used for further investigation.

4.3.5. Effect of reduced Vs. non-reduced single-site Co^{2+} heterogeneous catalyst

The reaction using cyclohexane conversion over reduced and non-reduced Co^{2+}/SiO_2 ($[Co(NH_3)_6]Cl_3$ as a precursor) were investigated, as shown in **Figure 4.8**.

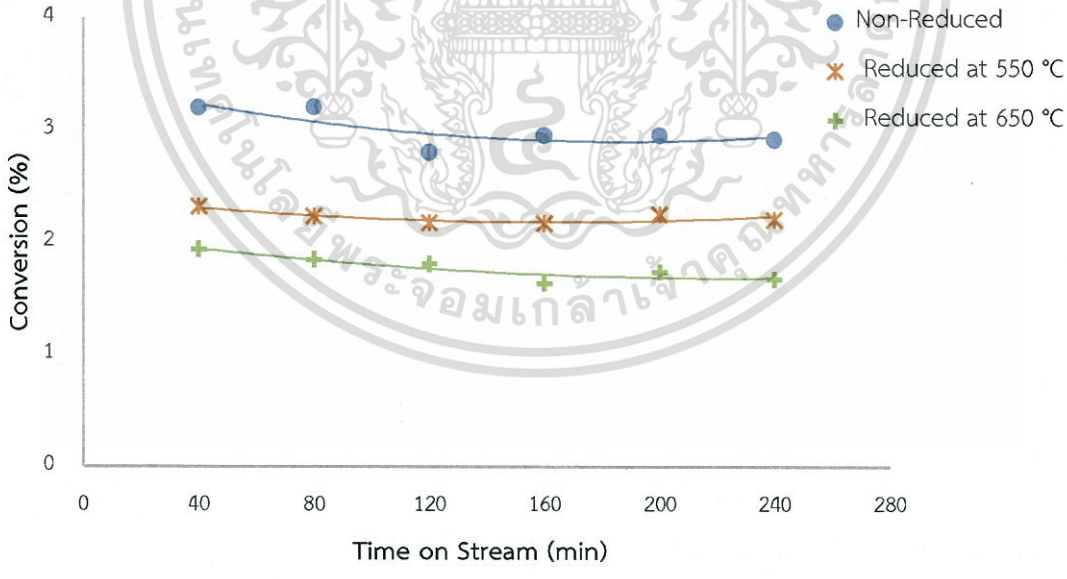

Figure 4.8 Conversion of cyclohexane by non-reduced and reduced catalysts (Reaction condition; Temperature: 550 °C, Pressure: 1 atm, Contact time: 36 g.h/mol, Flow rate of N_2 carrier gas 60 mL/min, Results at 240 minutes of time on stream)

Upon reducing cobalt, the cyclohexane conversion is decreased. It is decreased from 3.0% (non-reduced), 2.2% (reduced at 550 °C) to 1.8% (reduced at 650 °C). This indicates that the Co^{2+} is more active than metallic cobalt. The selectivity towards each product over non-reduced and reduced catalysts are summarized in **Table 4.5**.

Table 4.5 Selectivity toward each products over non-reduced and reduced catalysts

Catalysts	Conversion (%)	Selectivity of products (%)		
		Ethylene	Cyclohexene	Benzene
Non-Reduced	3.0	-	72.8	27.2
Reduced at 550°C	2.2	-	84.4	15.6
Reduced at 650°C	1.8	-	88.1	11.9

(Reaction condition; Temperature: 550 °C, Pressure: 1 atm, Contact time: 36 g.h/mol, Flow rate of N_2 carrier gas 60 mL/min, Results at 240 minutes of time on stream)

According to **Table 4.5**, the selectivity to cyclohexene is increased with reduction temperature. However, these changes in product selectivity may be derived from the change in conversion. Hence, the reaction at the same conversion. It test, as shown in **Table 4.6**.

Table 4.6 Selectivity towards each product by non-reduced and reduced catalysts

Catalyst	Conversion (%)	Contact time (g.h/mol)	Selectivity of products (%)		
			Ethylene	Cyclohexene	Benzene
Non-Reduced	3.4	42	-	71.3	28.7
Reduced at 550°C	3.4	54	-	68.8	31.2

(Reaction condition; Temperature: 550 °C, Pressure: 1 atm, Conversion: 3.39%, Flow rate of N_2 carrier gas 60 mL/min, Average Results at 200 minutes of time on stream)

According to **Table 4.6**, the selectivity of products are not much different. Hence, the non-reduced Co^{2+}/SiO_2 were used for further study.

4.3.6. Effect of metal precursor

The effect of using various cobalt complexes as a precursor ($[Co(NH_3)_6]Cl_3$, $[Co(NH_3)_5Cl]Cl_2$, $[Co(en)_2Cl_2]Cl$ and $[Co(bipy)_3](NO_3)_2$) compared with the impregnation of $Co(NO_3)_2.6H_2O$ method were investigated. The catalysts are weighed by same Co weight of each catalysts. The cyclohexane conversion at temperatures 550 and 600°C were studied.

Since loading of Co in each catalyst not the same, the catalyst was packed in a bed to keep the same Cobalt. In order to have the same amount of active site, the data from TPR were used to calculate the amount of cobalt in each bed catalyst. **Figure 4.9** shows the conversion of cyclohexane at 550 (A) and 600°C (B) by using various cobalt complex precursor.

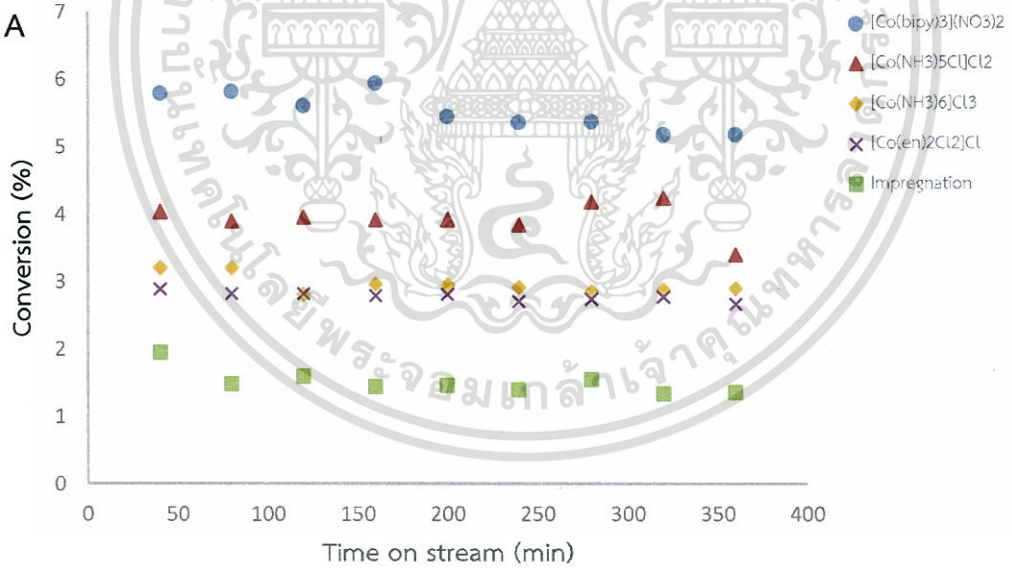

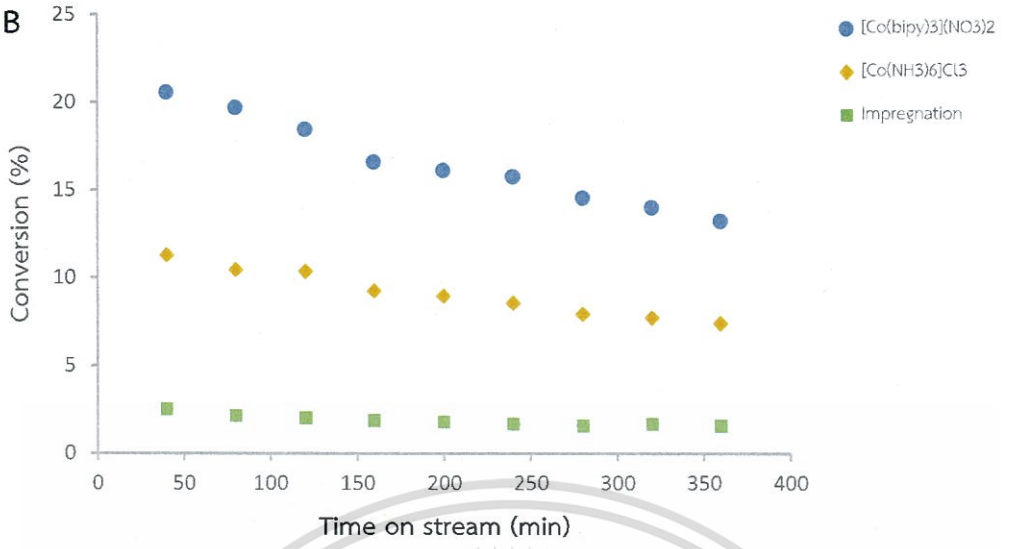

Figure 4.9 Conversion at 550 (A) and 600 °C (B) by using various cobalt complexes as a precursor : $[Co(NH_3)_6]Cl_3$ (♦), $[Co(NH_3)_5Cl]Cl_2$ (▲), $[Co(en)_2Cl_2]Cl$ (X), $[Co(bipy)_3](NO_3)_2$ (●) , Impregnation (■) catalyst (Reaction condition; Temperature: 550 °C, Pressure: 1 atm, Weight of Co: 2.26 mg., Flow rate of N_2 carrier gas 60 mL/min, Results at 360 minutes of time on stream)

According to **Figure 4.9A**, it is clearly seen that using the different cobalt complex precursors yielding the different conversion. The activity of the catalysts is in the order of $[Co(bipy)_3](NO_3)_2$ > $[Co(NH_3)_5Cl]Cl_2$ > $[Co(NH_3)_6]Cl_3$ > $[Co(en)_2Cl_2]Cl$. This tread is similar at reaction temperature 600 °C (**Figure 4.9B**). This can be explained that using the different cobalt complex precursors give the different dispersion, as demonstrated by **Figure 4.10**.

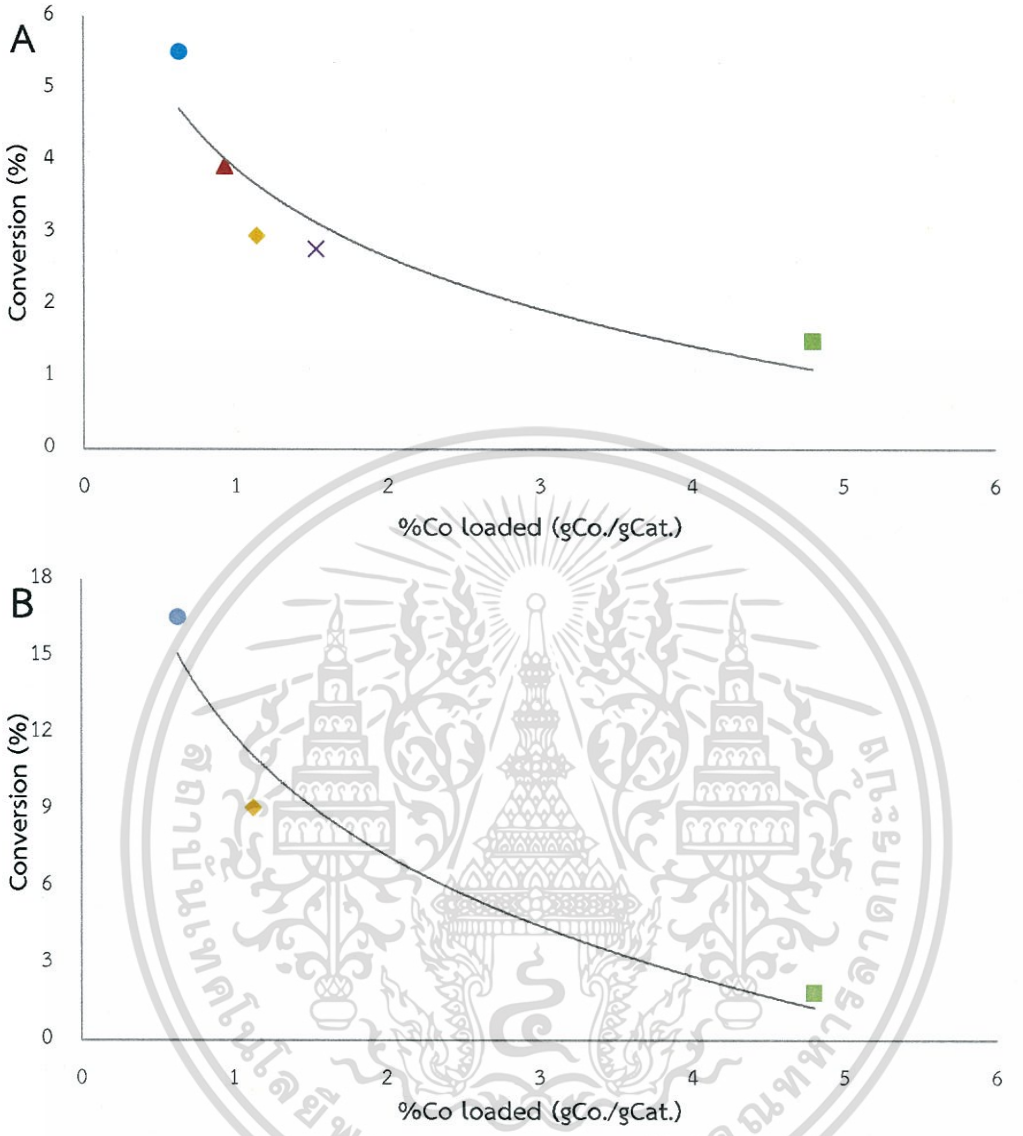

Figure 4.10 Conversion of cyclohexane Vs. %Co loading at 550 (A) and 600 °C (B) by using various cobalt complexes as a precursor : $[Co(NH_3)_6]Cl_3$ (◆), $[Co(NH_3)_5Cl]Cl_2$ (▲), $[Co(en)_2Cl_2]Cl$ (X), $[Co(bipy)_3](NO_3)_2$ (●), Impregnation (■) catalyst

According to **Figure 4.10**, the conversion of cyclohexane is decreased when the Co loading is increased for the reaction as 550 and 600 °C. This can be explained that the Co loading affects the dispersion. As the Co loading is increased the dispersion of cobalt could also be decreased. The selectivity of each catalyst at reaction temperature 550 and 600 °C Vs. conversion of cyclohexane are shown in **Figure 4.11**.

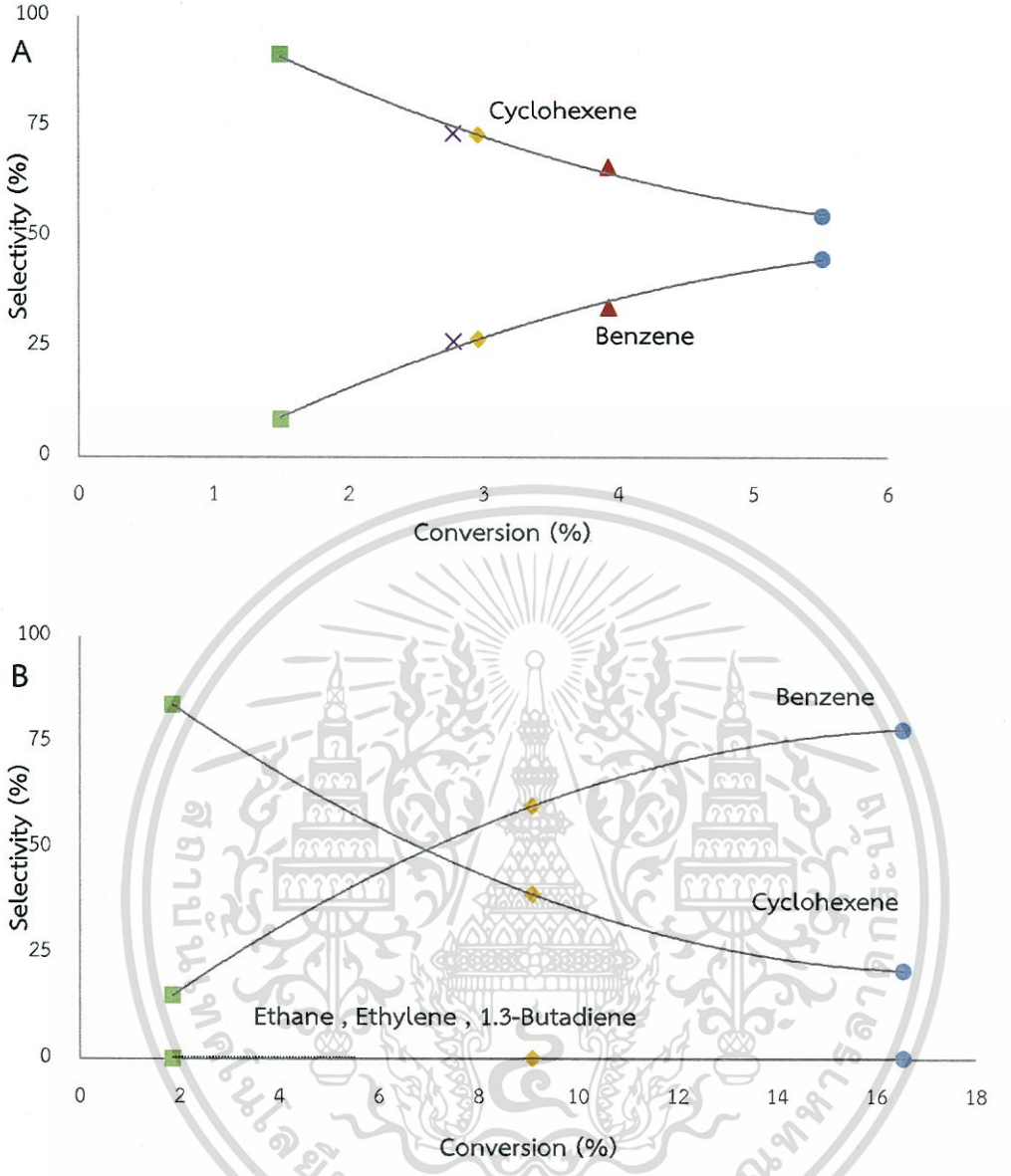

Figure 4.11 The selectivity Vs. conversion of cyclohexane at 550 (A) and 600 °C (B) by using various cobalt complexes as a precursor : $[Co(NH_3)_6]Cl_3$ (♦), $[Co(NH_3)_5Cl]Cl_2$ (▲), $[Co(en)_2Cl_2]Cl$ (X), $[Co(bipy)_3](NO_3)_2$ (●), Impregnation (■) catalyst

According to **Figure 4.11**, the selectivity of benzene is increased. While, the selectivity of cyclohexene is decreased. It is suggested that increasing the dispersion of cobalt on catalyst. it is increased the conversion.

the cracking products including, benzene, ethylene, ethane and 1,3-butadiene is increased with the conversion for the reaction as 550 and 600 °C.

4.3.7. Deactivation of catalysts

The deactivation of catalysts preparing from impregnation and adsorption using $[Co(bipy)_3](NO_3)_2$ as a precursor was investigated. In order to compare the behavior of the deactivation, the amount of Co in the impregnation was increased 8 times than the catalysts prepared by the adsorption.

In order to investigate the ability of regeneration of the catalyst, the used catalyst was treated in air for 5 hours after running the reaction for 6 hours at the same temperature. The conversion of cyclohexane is represented in **Figure 4.12**.

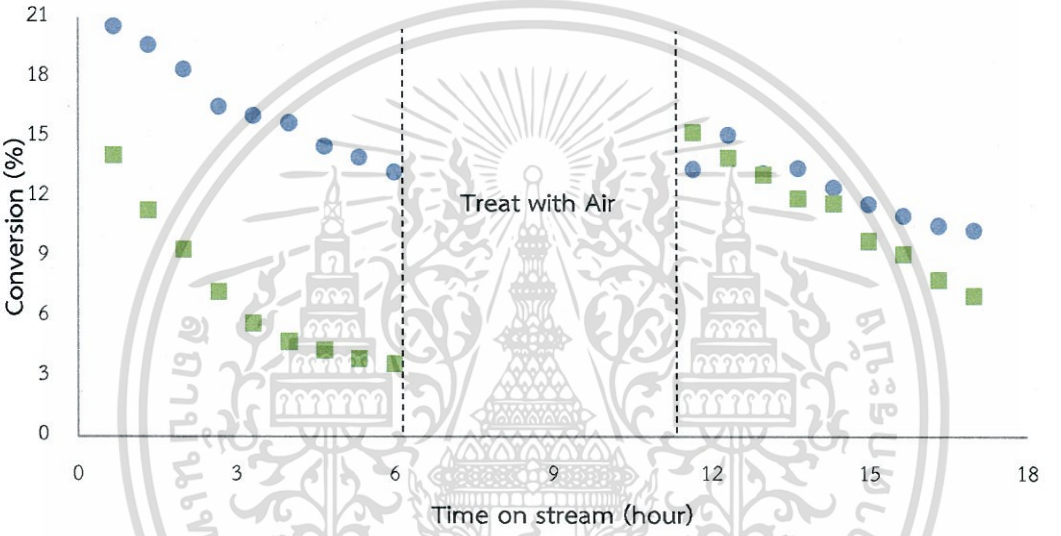

Figure 4.12 Conversion of cyclohexane by using $[Co(bipy)_3](NO_3)_2$ (●), Impregnation (■) catalyst (Reaction condition; Temperature: 600 °C, Pressure: 1 atm, Weight of Co: 2.26 mg., Flow rate of N_2 carrier gas 60 mL/min, Results at 360 minutes of time on stream)

Upon running the reaction for longer time, the activity of catalysts is deceased. Then, after running the reaction for 6 hours, the catalysts was treated with air for 5 hours at 600 °C in order to decomposes the coke. After that, nitrogen was fed for 30 minutes for reactivate. Then, cyclohexane was fed on the reaction was monitored. It can be seen that the catalyst was prepared by adsorption technique, the conversion is not, as high as the fresh catalysts could be caused metal denature of the catalysts. However, the catalyst was prepared by the impregnation method, the conversion is, as high as the fresh catalysts could be caused coke formation.

CHAPTER 5
CONCLUSION AND SUGGESTION

5.1 Conclusions

In this project, the dehydrogenation of cyclohexane was studied over single-site Co^{2+}/SiO_2 catalysts and non-single-site Co/SiO_2 catalyst. The catalysts preparation by electrostatic adsorption methodology using $[Co(bipy)_3](NO_3)_2$, $[Co(NH_3)_5Cl]Cl_2$, $[Co(NH_3)_6]Cl_3$ and $[Co(en)_2Cl_2]Cl$ as a precursor were compared impregnation method using $Co(NO_3)_2.6H_2O$ as a precursor, were characterized using Ultraviolet–Visible spectroscopy (UV-Vis), Temperature programmed reduction (TPR) and Inductively coupled plasma mass spectrometry (ICP-MS) techniques confirming the Co loading. The non-single-site cobalt can be prepared by the impregnation method. It can create the highest cobalt loading as non-single-site species and single-site species. However, the adsorption technique gives pure single-site cobalt. From the results of all techniques, the cobalt loading is increased from $[Co(bipy)_3](NO_3)_2$ < $[Co(NH_3)_5Cl]Cl_2$ < $[Co(NH_3)_6]Cl_3$ < $[Co(en)_2Cl_2]Cl$. Hence, the adsorption technique depends on the charge density of the precursor. However, *tran*-$[Co(en)_2Cl_2]Cl$ is an exception because it could have a better geometry to interact with the negative charge on the silica surface, as compared to other cobalt complexes.

The dehydrogenation of cyclohexane results in cyclohexene that can be dehydrogenated to benzene. However, benzene is also obtained in parallel reaction from direct conversion of cyclohexane. Moreover, ethylene, ethane and 1,3-butadiene could be derived from cyclohexene due to thermal cracking at high temperature (>550 °C). In addition, ethylene could be hydrogenated to ethane.

As the contract time and temperature are increased, rate of the reaction is increased. However, product selectivity was modified by conversion. The optimum contract time for the dehydrogenation of cyclohexane to cyclohexene (to obtain higher cyclohexene selectivity) is 36 g.h/mol. At higher contract time (i.e. 144 g.h/mol), cyclohexene can be easily dehydrogenated to benzene.

For the comparison under N_2 and H_2 atmosphere, using H_2 as a carrier gas could lead to the formation of cobalt hydride. It could lead to cobalt hydride that possesses

higher activity, as compared to single-site cobalt. However, using N_2 as a carrier gas gives higher cyclohexene selectivity.

The reduced single-site Co^{2+} gives a lower cyclohexane conversion. This is because Co^{2+} is more active than metallic cobalt. Comparing as the same conversion, the selectivity in the same.

As compared the activity of metal precursor, the activity for the dehydrogenation of cyclohexane is in the order of $[Co(bipy)_3](NO_3)_2$ > $[Co(NH_3)_5Cl]Cl_2$ > $[Co(NH_3)_6]Cl_3$ > $[Co(en)_2Cl_2]Cl$ > $Co(NO_3)_2.6H_2O$. This can be explained that using the different metal precursor give the different dispersion. For impregnation method shows dramatically lower conversion. This indicates that the impregnation method gives low dispersion, presumable due to accommodation of the cobalt metal.

5.2 Suggestions

5.2.1) In order to obtain high conversion of cyclohexane to benzene, using higher contract time, temperature reaction and mixed carrier gas H_2/N_2 should be considered.

5.2.2) In order to study the single-site cobalt catalyst can react aromatization reaction well, changing the feed of reaction to alkanes are interested.

REFERENCES

[1] Nagahara H., Ono M., Konishi M. and Fukuoka Y. 1997. "**Partial hydrogenation of benzene to cyclohexene.**" Applied Surface Science. 121/122 : 448-451.

[2] AbdelDayem H. M., Faiz M., Abdel-Samad H. S. and Hassan S. A. 2015. "**Rare earth oxides doped NiO/ γ -Al_2O_3 catalyst for oxidative dehydrogenation of cyclohexane.**" Journal of Rare Earths. 33 : 611.

[3] Goergen S., et al. 2013. "**Structure Sensitivity of Oxidative Dehydrogenation of Cyclohexane over FeO_x and Au/Fe_3O_4 Nanocrystals.**" ACS Catalysis. 3 : 529-539.

[4] Tyo E. C., et al. 2012. "**Oxidative Dehydrogenation of Cyclohexane on Cobalt Oxide (Co_3O_4) Nanoparticles: The Effect of Particle Size on Activity and Selectivity.**" ACS Catalysis. 2 : 2409-2423.

[5] Furukawa S., Tamura A., Ozawa K. and Komatsu T. 2014. "**Catalytic properties of Pt-based intermetallic compounds in dehydrogenation of cyclohexane and n-butane.**" Applied Catalysis A: General. 469 : 300-305.

[6] Alia L. I., et al. 1999. "**Dehydrogenation of cyclohexane on catalysts containing noble metals and their combinations with platinum on alumina support.**" Applied Catalysis A: General. 177 : 99–110.

[7] Nai-liang W., et al. 2015. "**Effect of microwave calcination on catalytic properties of Pt/MgAl(Sn)O_x catalyst in cyclohexane dehydrogenation to cyclohexene.**" Applied Catalysis A: General. 503 : 62-68.

[8] Wang Y., Shah N., and Huffman G. P. 2004. "**Pure Hydrogen Production by Partial Dehydrogenation of Cyclohexane and Methylcyclohexane over Nanotube-Supported Pt and Pd Catalysts.**" Energy & Fuels. 18 : 1429-1433.

[9] Li J., et al. 2014. "**The catalytic performance of Ni_2P/Al_2O_3 catalyst in comparison with Ni/Al_2O_3 catalyst in dehydrogenation of cyclohexane.**" Applied Catalysis A: General. 469 : 434-441.

[10] Escobar J., et al. 2006. "**Cyclohexane Dehydrogenation over Wet-Impregnated Ni on Al_2O_3-TiO_2 Sol-Gel Oxides.**" Industrial & Engineering Chemistry Research. 45 : 5693-5700.

[11] Seemeyer K., et al. 1995. "**Face Selectivity of the C-H Bond Activation of Cyclohexane by the "Bare" First-Row Transition-Metal Cations Sc^{+}-Zn^{+}.**" Organometallics. 14 : 4465-4470

[12] Hu B., et al. 2015. "**Selective propane dehydrogenation with single-site Co^{II} on SiO_2 by a non-redox mechanism.**" Journal of Catalysis. 322 : 24–37.

[13] Schweitzer N. M., et al. 2014. "**Propylene Hydrogenation and Propane Dehydrogenation by a Single-Site Zn^{2+} on Silica Catalyst**" ACS Catalysis. 4 : 1091–1098.

[14] Farnetti E., Monte R. D. and Kaspar J. "**Homogeneous and Heterogeneous Catalysis.**" Inorganic and Bio-Inorganic Chemistry. 2.

[15] **Basset J.M., et al. 2010. "Metathesis of Alkanes and Related Reactions." Accounts of Chemical Research. 43 : 323–334.**

[16] Dufaud V., et al. 1995. "**Surface Organometallic Chemistry of Inorganic Oxides: The Synthesis and Characterization of $(\equiv SiO)Ta(=CHC(CH_3)_3)(CH_2C(CH_3)_3)_2$ and $(\equiv SiO)_2Ta(=CHC(CH_3)_3(CH_2C(CH_3)_3.$**" Journal of the American Chemical Society. 117 : 4288–4294.

[17] Harry W. H., 1962. "**The trend is toward hydrogenation high purity for a billion-pound-per-year market**" Industrial and Engineering Chemistry 54(7) : 23-30

[18] Billaud F., Chaverot P., Berthelin M. and Freundg E. 1988. "**Thermal Decomposition of Cyclohexane at Approximately 810 °C.**" Industrial & Engineering Chemistry Research. 27 : 759-764.

[19] Jian-ping D., et al. 2015. "**Cyclohexane dehydrogenation over the platinum catalysts supported on carbon nanomaterials.**" Journal of Fuel Chemistry and Technology. 37(4) : 468-472.

[20] Infrared and Raman Spectra of Inorganic andCoordination Compounds. [Online]. Available : http://samples.sainsburysebooks.co.uk/9780470405871_sample_382833.pdf

[21] Asewave K., Yiase S.G., Adejo S. O. and Anhwange B. A. 2012. "**Substitution Reaction of *trans*-dichloro-*bis*-(ethylenediamine)Cobalt (III) Chloride and**

Phenylalanine - A Kinetics and Mechanism Study." International Journal of Modern Chemistry. 1(2) : 93-101.

[22] Chuy C., Falvello L. R., Libby E., Santa-Maroa J. C. and Tomas M. 1997. "**Complexes of the Trioxodinirrate Anion: Synthesis and Characterization of [Zn(II)(bipy)(H_2O)(N_2O_3)] and [Co(II)(bipy)$_2$(N_2O_3)].**" Inorganic Chemistry 36 : 2004-2009.

[23] **Synthesis of Hexaammine Cobalt(III) Chloride.** [Online]. Available : http://rexresearch.com/cohex/hexaammine.pdf

[24] **Preparation of *trans*-[$CoCl_2$(en)$_2$]Cl.** [Online]. Available : http://wwwchem.uwimona.edu.jm/lab_manuals/c21jexpt.html

[25] **Transition Metal Complexes and Color.** [Online]. Available : https://www.wou.edu/las/physci/ch462/tmcolors.htm

[26] Sharma R. P., Sharma R., Bala R., Salas J. M. and Quiros M. 2006. "**Second sphere coordination complexes via hydrogen bonding: Synthesis, spectroscopic characterization of [*trans*-Co(en)$_2$$Cl_2$]$CdX_4$ (X=Br or I) and single crystal X-ray structure determination of [*trans*-Co(en)$_2$$Cl_2$]$CdBr_4$.**" Journal of Molecular Structure. 794 : 341-347.

[27] Hugo A. O., et al. 2012. "**Support effect on carbon nanotube growth by methane chemical vapor deposition on cobalt catalysts**" Journal of the Brazilian Chemical Society. 23(5) : 868-879.

[28] Gendt S. D., et al. 2009. "**Atomic Layer Deposition Applications 5.**" ECS Transactions. 25(4) : 49-55.

[29] Hou K. C. and Palmer H. B. 1965. "**The Kinetics of Thermal Decomposition of Benzene in a Flow System.**" Journal of Physical Chemistry. 69(3) : 863-868.

[30] Jame S. 2005. "**Lange's Handbook of Chemistry, Sixteenth Edition.**"

[31] Chase, M.W. and Jr. 1998. "***NIST-JANAF Themochemical Tables, Fourth Edition.***" Journal of Physical and Chemical Reference Data, **Monograph 9 :** 1-1951.

[32] Kayode C. 2007. "**Ludwig's Applied Process Design for Chemical and Petrochemical Plants, Volume 1.**"

APPENDICES

APPENDIX A

ULTRAVIOLET-VISIBLE REFERENCE

A1. Calibration of $[Co(NH_3)_6]Cl_3$

The UV-Vis absorption of $[Co(NH_3)_6Cl_3$ in aqueous solution at pH 11 and *different concentrations* were depicted by :

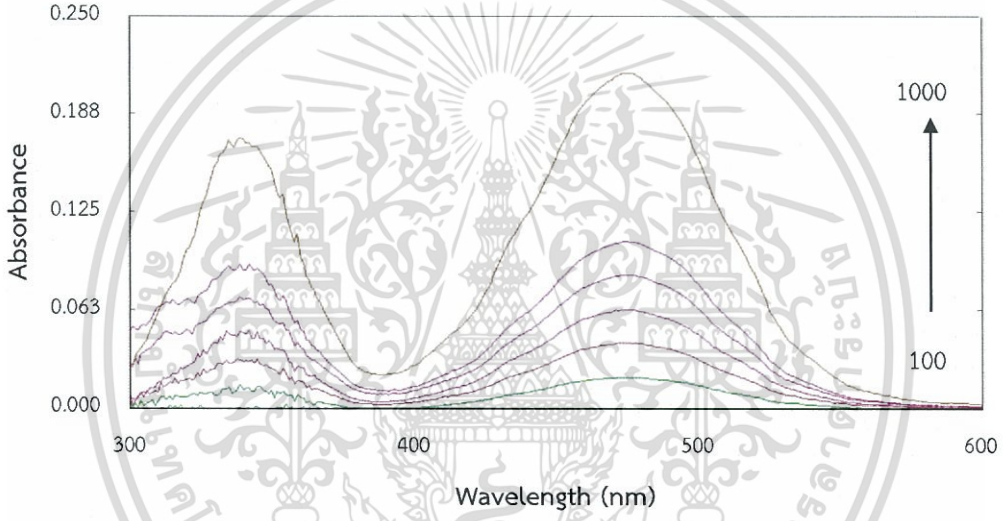

Figure A1. UV-Vis Absorption of $[Co(NH_3)_6]Cl_3$ at *different concentrations*; the bottom to top line is 100, 200, 300, 400, 500 and 1000 ppm, respectively.

In order to determine %Co loading on silica, the UV-Vis absorption calibration curve of $[Co(NH_3)_6]Cl_3$ at λ_{max}= 475 nm is shown in **Figure A2**.

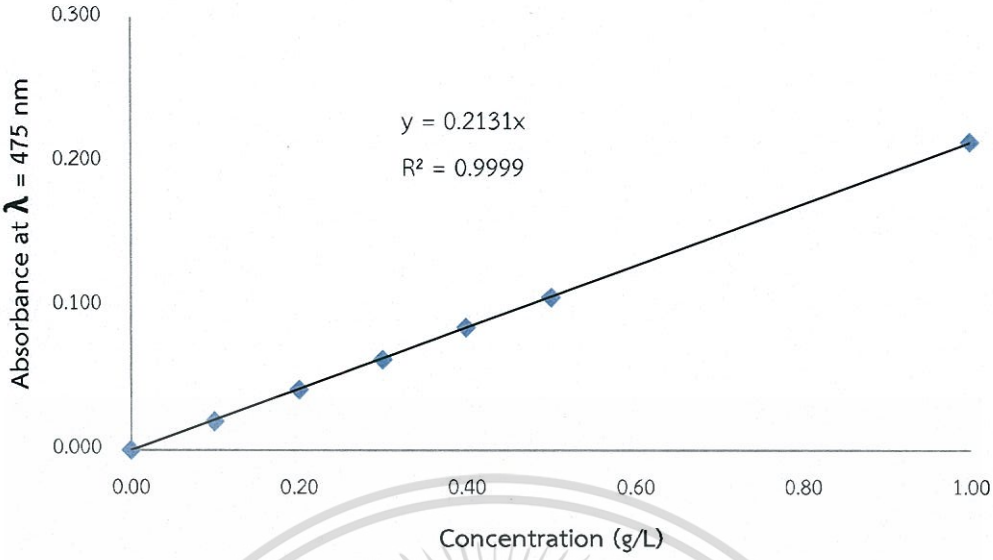

Figure A2 UV-Vis Absorption calibration curve of $[Co(NH_3)_6]Cl_3$

For the example, the standard cobalt complex solution value (y) ; 0.025 Abs.

$$x = \frac{y}{0.2131}$$

$$= \frac{0.025}{0.2131}$$

$$= 0.1173$$

Due to the standard solution cobalt complex was diluted by 10 times. Thus, the standard cobalt solution ;

$$\text{The standard cobalt solution} = \frac{(10)(x)}{\text{molecular weight of complex}}$$

$$= \frac{(10)(0.1173)(1000)}{267.43}$$

$$= 4.3868 \text{ mmol}$$

The remain solution cobalt complex value (y) ; 0.018 Abs.

$$x = \frac{y}{0.2131}$$

$$= \frac{0.018}{0.2131}$$

$$= 0.0845$$

Due to the remain solution cobalt complex was diluted by 10 times. Thus, the remain cobalt solution ;

$$\text{The remain cobalt solution} = \frac{(10)(x)}{\text{molecular weight of complex}}$$

$$= \frac{(10)(0.845)(1000)}{267.43}$$

$$= 3.1584 \text{ mmol}$$

A2. Calibration of $[Co(NH)_5Cl]Cl_2$

The UV-Vis absorption of $[Co(NH_3)_5Cl]Cl_2$ in aqueous solution at pH 11 and *different concentrations* were depicted by :

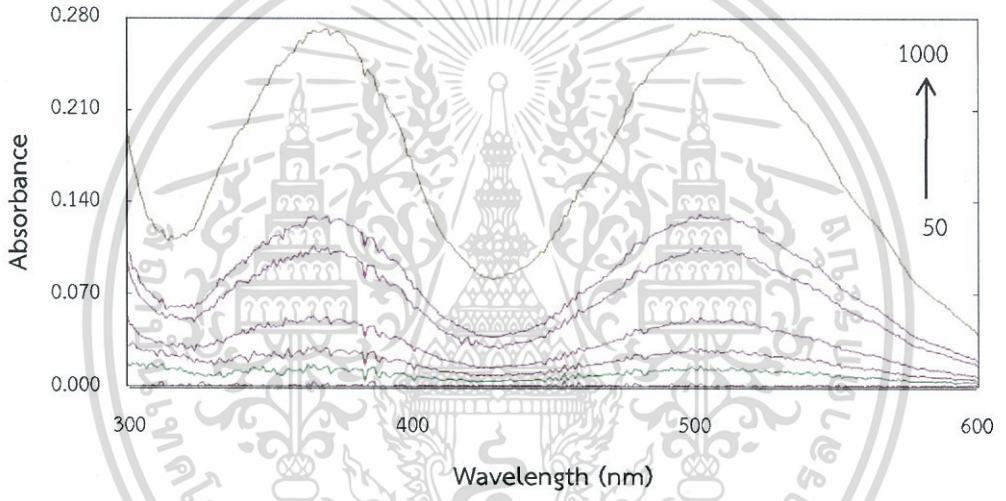

A3. UV-Vis Absorption of $[Co(NH_3)_5Cl]Cl_2$; the bottom to top line is 50, 100, 200, 400, 500 and 1000 ppm, respectively.

In order to determine %Co loading on silica, the UV-Vis absorption calibration curve of $[Co(NH_3)_5Cl]Cl_2$ at λ_{max}= 502 nm is shown in **A4**.

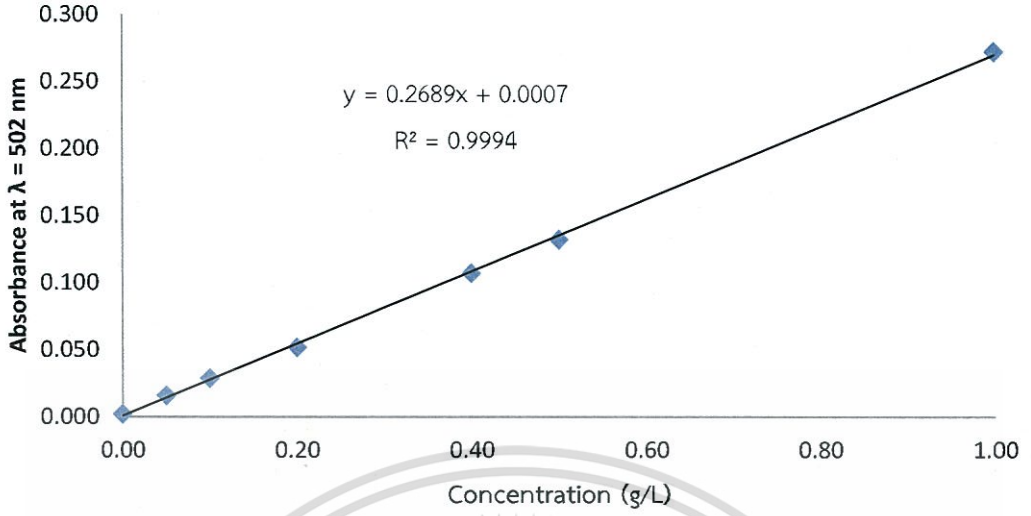

A4. UV-Vis Absorption calibration curve of $[Co(NH_3)_5Cl]Cl_2$

The standard cobalt complex solution value (y) ; 0.032 Abs., which corresponds to ; x = 0.1164 g/L.

Due to the standard solution cobalt complex was diluted by 10 times. Thus, the standard cobalt solution = 4.6480 mmol

The remain solution cobalt complex value (y) ; 0.027 Abs., which corresponds to ; x = 0.0978 g/L.

Due to the remain solution cobalt complex was diluted by 10 times. Thus, the remain cobalt solution = 3.9055 mmol

A3. Calibration of $[Co(en)_2Cl_2]Cl$

The UV-Vis absorption of $[Co(en)_2Cl_2]Cl$ in aqueous solution at *different concentrations* is shown in **A5.**

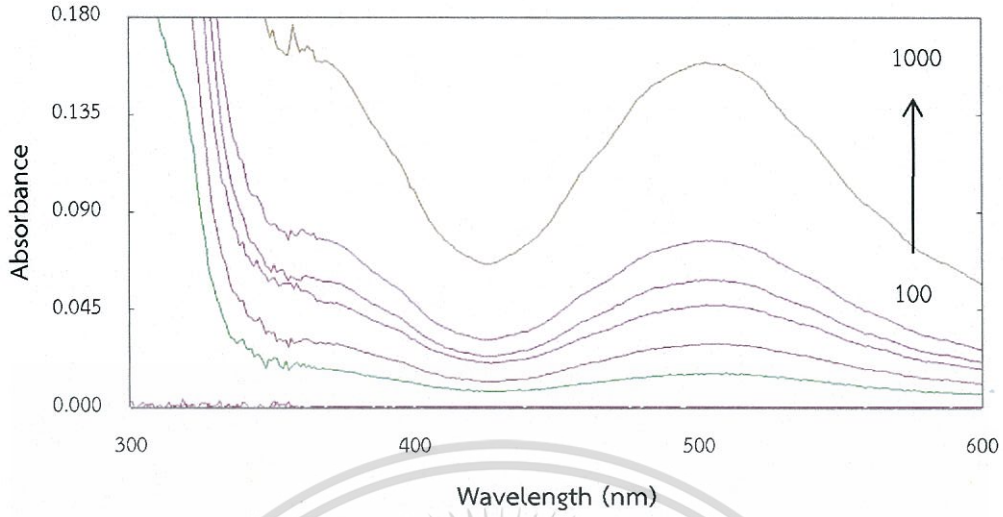

A5. UV-Vis Absorption of $[Co(en)_2Cl_2]Cl$; the bottom to top line is 100, 200, 300, 400, 500 and 1000 ppm, respectively.

In order to determine %Co loading on silica, the UV-Vis absorption calibration curve of of $[Co(en)_2Cl_2]Cl$ at λ_{max}= 500 nm is shown in **A6**.

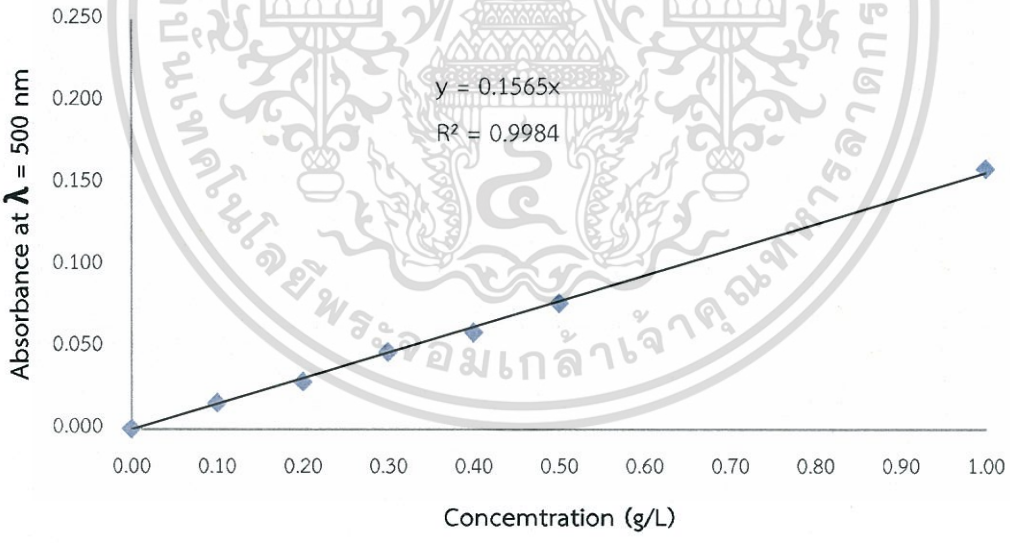

A6. UV-Vis Absorption calibration curve of $[Co(en)_2Cl_2]Cl$

The standard cobalt complex solution value (y) ; 0.021 Abs., which corresponds to ; x = 0.1342 g/L.

Due to the standard solution cobalt complex was diluted by 10 times. Thus, the standard cobalt solution = 5.0176 mmol

Due to the red shifts of λ_{max} of the $[Co(en)_2Cl_2]Cl$ remain solution, %Co loading using this precursor cannot be analyzed by UV-Vis as shown in **A7**.

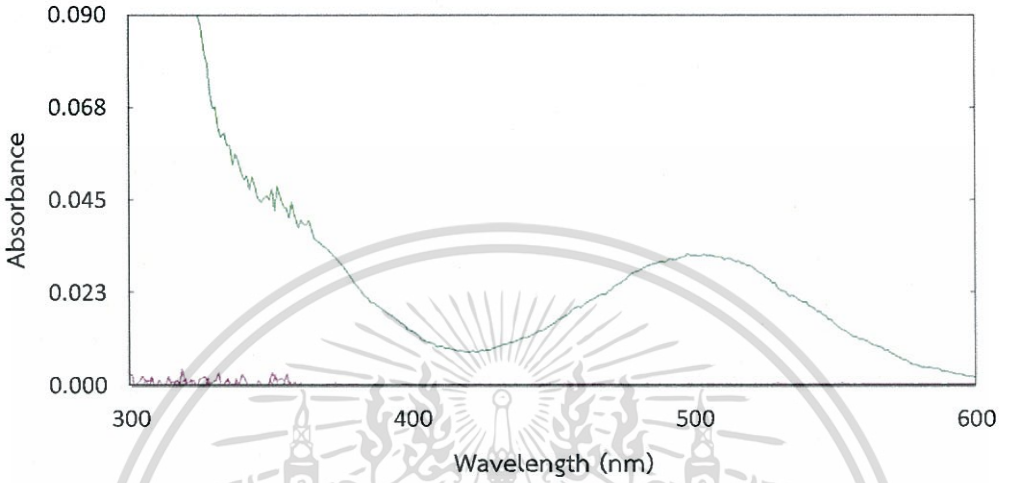

A7. UV-Vis Absorption of the $[Co(en)_2Cl_2]Cl$ remain solution dilute by 10 times

The $[Co(en)_2Cl_2]Cl$ remain solution shows the UV-Vis absorption at λ_{max}= 505 nm : while the UV-Vis absorption of $[Co(en)_2Cl_2]Cl$ shows λ_{max}= 500 nm.

A4. Calibration of $[Co(bipy)_3](NO_3)_2$

The UV-Vis absorption of $[Co(bipy)_3](NO_3)_2$ in aqueous solution at pH 11 and *different concentrations* is shown in **A8**.

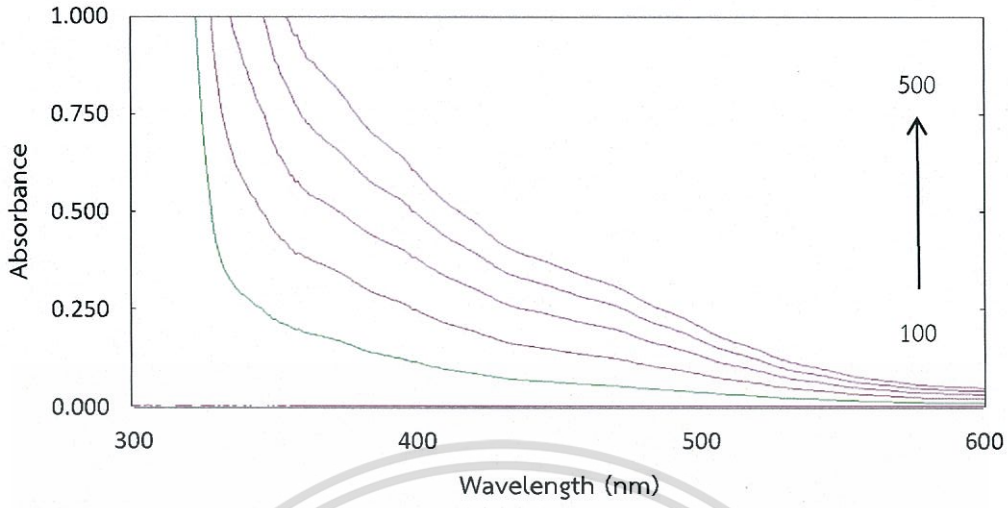

A8. UV-Vis Absorption of $[Co(bipy)_3](NO_3)_2$; the bottom to top line is 100, 200, 300, 400 and 500 ppm, respectively.

In order to determine %Co loading on silica, the UV-Vis absorption calibration curve of $[Co(bipy)_3](NO_3)_2$ at λ= 438nm is shown in **A9**.

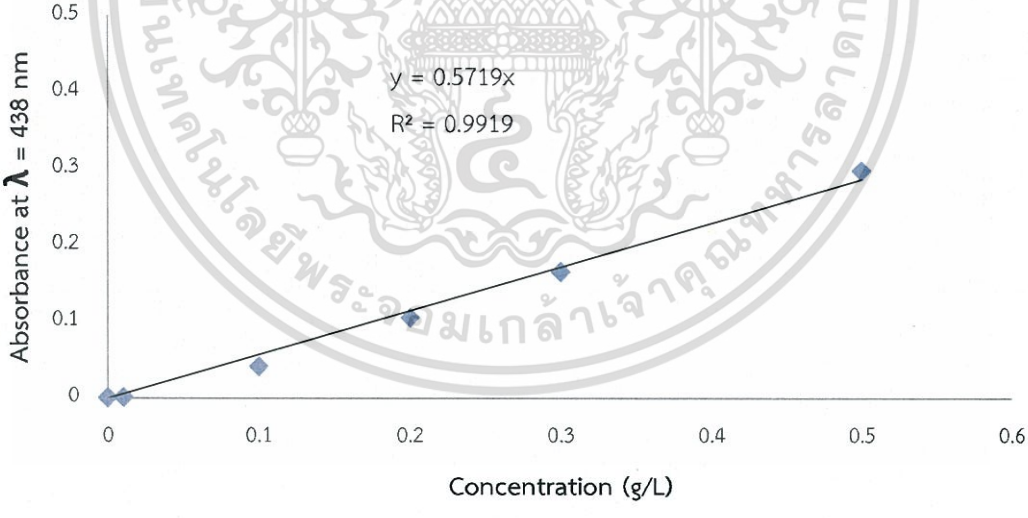

A9. UV-Vis Absorption calibration curve of $[Co(bipy)_3](NO_3)_2$

The standard cobalt complex solution value (y) ; 0.127 Abs., which corresponds to ; x = 0.1587 g/L.

Due to the standard solution cobalt complex was diluted by 25 times. Thus, the standard cobalt solution = 6.0940 mmol

The remain solution cobalt complex value (y) ; 0.123 Abs., which corresponds to ; x = 0.1537 g/L.

Due to the remain solution cobalt complex was diluted by 25 times. Thus, the remain cobalt solution = 5.9021 mmol

APPENDIX B

INFARED SPECTRA REFERENCE

Table B1. IR spectra of hexaamminecobalt(III) chloride ($[Co(NH_3)_6]Cl_3$).[20]

Wavenumber (cm^{-1})	Vibration mode
833	N-H bending
1328	N-H bending
1620	N-H bending
3179	N-H stretching
3245	N-H stretching

Table B2. IR spectra of pentaamminechlorocobalt(III) chloride($[Co(NH_3)_5Cl]Cl_2$).[20]

Wavenumber (cm^{-1})	Vibration mode
489	Metal-N
858	N-H bending
1319	N-H bending
1610	N-H bending
3132	N-H stretching
3671-3325	O-H stretching

Table B3. IR spectra of *trans*-dichloro-*bis*-(ethylenediamine)cobalt(III) chloride ($[Co(en)_2Cl_2]Cl$).[21]

Wavenumber (cm^{-1})	Vibration mode
474	Metal-N
888	N-H bending
1053	C-N stretching
1115	C-N stretching
1206	C-N stretching
1314	N-H bending

1445	C-H bending
1594	N-H bending
2954	C-H stretching
3220	N-H stretching
3741-3316	O-H stretching

Table B4. IR spectra of *tris*-(bipyridine)cobalt(II) nitrate ($[Co(bipy)_3](NO_3)_2$).[21]

Wavenumber (cm^{-1})	Vibration mode
419	Metal-N
652	C-C out-of-plane deformation
737	C-H out-of-plane deformation
784	C-H out-of-plane bending
827	C-H out-of-plane bending
911	C-H out-of-plane bending
1019	C-H bending
1064	C-H bending
1104	C-H bending
1162	C-H bending
1251	C-N stretching
1316	C-N stretching
1395	C-N stretching
1446	C=N stretching
1475	C=N stretching
1493	C=C stretching
1599	C=C stretching
3075	C-H Stretching
3709-3163	O-H stretching

APPENDIX C
GAS CHROMATOGRAM

C. 1 Analysis of product from gas chromatography

The quantitative analysis of each products was detected by GC-FID (gas chromatography with flam ionization detector) with the condition in **Table C1**

Table C1 The GC condition for quantitative analysis

Column	EQUITY™-1
Temperature program	35 °C (9 min hold) to 100 °C (30 sec hold) at 15 °C/min to 220 °C at 15 °C/min
Carrier gas	Nitrogen at 60 mL/min
Injaction	550 °C
Detector	FID

The chromatography of products were identified using reference standard for comparison in **Table C2**

Table C2 Chromatogram data of standard product distribution and feed

Product or feed	Retention time of standard (min)
Ethylene	1.6
Ethane	2.3
1,3-Butadiene	4.3
Benzene	9.8
Cyclohexane	10.5
Cyclohexene	11.1

APPENDIX D

REACTION DATA

Table D1 Product yields reduced and non-reduced of $[Co(NH_3)_6]Cl_3$ at temperature 550°C

Catalyst	Time (h)	Conversion (%)	Yield (%)				
			Ethylene	Ethane	1,3-Butadiene	Benzene	Cyclohexene
Non-Reduced	6	3.01	0	0	0	0.82	2.19
Reduced at 550°C	6	2.22	0	0	0	0.35	1.87
Reduced at 650°C	6	1.77	0	0	0	0.21	1.56

Table D2 Product yields at temperature 550°C

Catalyst	Time (h)	Conversion (%)	Yield (%)				
			Ethylene	Ethane	1,3-Butadiene	Benzene	Cyclohexene
Blank	6	0	0	0	0	0	0
$[Co(NH)_6]Cl3$	6	2.96	0	0	0	0.79	2.17
$[Co(NH_3)_5Cl]Cl_2$	6	3.93	0	0	0	1.34	2.59
$[Co(en)_2Cl_2]Cl$	6	2.77	0	0	0	0.73	2.05
$[Co(bipy)_3](NO_3)_2$	6	5.52	0	0	0	2.50	3.02
$Co(NO_3)_2.6H_2O$	6	1.50	0	0	0	0.13	1.37

Table D3 Product yields at temperature 600°C

Catalyst	Time (h)	Conversion (%)	Yield (%)				
			Ethylene	Ethane	1,3-Butadiene	Benzene	Cyclohexene
Blank	6	0.01	0.01	0	0	0	0
$[Co(NH)_6]Cl3$	6	9.09	0.02	0.03	0.02	5.51	3.50
$[Co(bipy)_3](NO_3)_2$	6	16.55	0.04	0.05	0.04	13.02	3.40
$Co(NO_3)_2.6H_2O$	6	1.87	0.01	0.01	0	0.30	1.55

APPENDIX E

GIBBS FREE ENERGY

E1. Gibbs free energy of cyclohexene hydrogenation and cyclohexane dehydrogenation

Table E1 Enthalpy and Entropy of formation for the products and reactants [30-31]

Compound	ΔH_f° (kJ/mol)	ΔS° (J/mol.K)
$C_6H_{12}(g)$	-123.0	298.0
$C_6H_{10}(g)$	-5.4	311.0
$H_2(g)$	0	130.7

$C_6H_{12}(g) \longrightarrow C_6H_{10}(g) + H_2(g)$

$\Delta H^\circ_{rxn} = \sum \Delta H_f^\circ_{products} - \sum \Delta H_f^\circ_{reactants}$

$\Delta H^\circ_{rxn} = \{(1\ mol)(H_f^\circ[C_6H_{10}(g)]) + (1\ mol)(H_f^\circ[H_2(g)])\} - \{(1\ mol)(H_f^\circ[C_6H_{12}(g)])\}$

$\Delta H^\circ_{rxn} = [(1\ mol)(-5.4\ kJ/mol) + (1\ mol)(0\ kJ/mol)] - [(1\ mol)(-123.0\ kJ/mol)]$

$\Delta H^\circ_{rxn} = 117.6\ kJ$

ΔH is positive. Therefore, the reaction is endothermic.

$\Delta S^\circ_{rxn} = \sum \Delta S^\circ_{products} - \sum \Delta S^\circ_{reactants}$

$\Delta S^\circ_{rxn} = \{(1\ mol)(S^\circ[C_6H_{10}(g)]) + (1\ mol)(S^\circ[H_2(g)])\} - \{(1\ mol)(S^\circ[C_6H_{12}(g)])\}$

$\Delta S^\circ_{rxn} = [(1\ mol)(311.0\ J/mol.K) + (1\ mol)(130.7\ J/mol.K)] - [(1\ mol)(298.0\ J/mol.K)]$

$\Delta S^\circ_{rxn} = (143.7\ J/K)(1\ kJ/1000J)$

$\Delta S°_{rxn}$ = 0.1437 kJ/K

$\Delta G°_{rxn} = \Delta H°_{rxn} - T\Delta S°_{rxn}$

$\Delta G°_{rxn}$ = (117.6 kJ) - (298.15K)(0.1437 kJ/K)

$\Delta G°_{rxn}$ = 74.74 kJ

ΔG is positive. Therefore, the reaction is not spontaneous.

$C_6H_{10}(g) + H_2(g) \longrightarrow C_6H_{12}(g)$

$\Delta H°_{rxn} = \sum \Delta H_f°_{products} - \sum \Delta H_f°_{reactants}$

$\Delta H°_{rxn}$ = {(1 mol)($H_f°[C_6H_{12}(g)]$)} - (1 mol)($H_f°[C_6H_{10}(g)]$) + (1 mol)($H_f°[H_2(g)]$)}

$\Delta H°_{rxn}$ = [(1 mol)(-123.0 kJ/mol)] - [(1 mol)(-5.4 kJ/mol) + (1 mol)(0 kJ/mol)]

$\Delta H°_{rxn}$ = -117.6 kJ

ΔH is negative. Therefore, the reaction is exothermic.

$\Delta S°_{rxn} = \sum \Delta S°_{products} - \sum \Delta S°_{reactants}$

$\Delta S°_{rxn}$ = {(1 mol)($S°[C_6H_{12}(g)]$)} - {(1 mol)($S°[C_6H_{10}(g)]$) + (1 mol)($S°[H_2(g)]$)}

$\Delta S°_{rxn}$ = [(1 mol)(298.0 J/mol.K)] - [(1 mol)(311.0 J/mol.K) + (1 mol)(130.7 J/mol.K)]

$\Delta S°_{rxn}$ = (-143.7 J/K)(1 kJ/1000J)

$\Delta S°_{rxn}$ = -0.1437 kJ/K

$\Delta G°_{rxn} = \Delta H°_{rxn} - T\Delta S°_{rxn}$

$\Delta G°_{rxn}$ = (-117.6 kJ) - (298.15K)(-0.1437 kJ/K)

$\Delta G°_{rxn}$ = -74.74 kJ

ΔG is negative. Therefore, the reaction is spontaneous.

The gibbs free energy of cyclohexene hydrogenation and cyclohexane dehydrogenation are negative were depicted by :

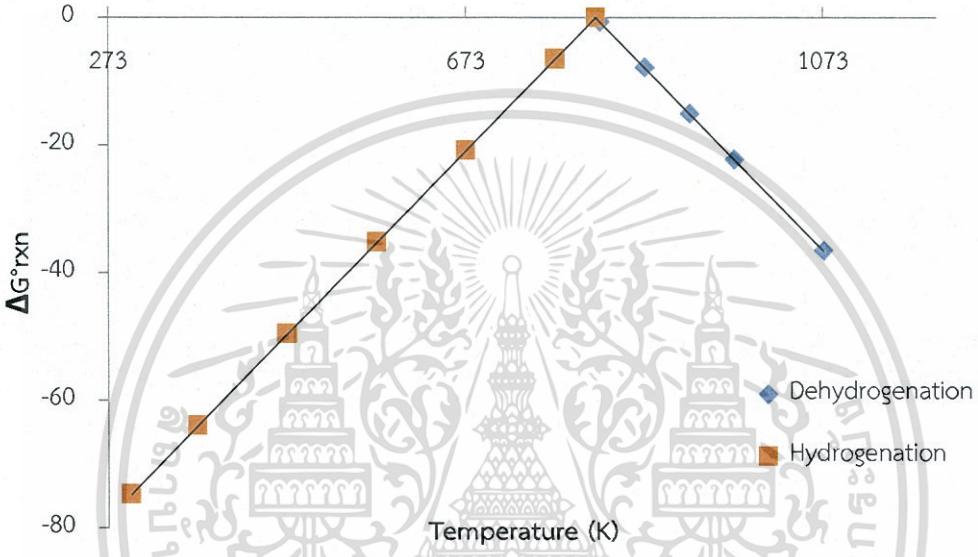

Figure E.1 Gibbs free energy various temperature of cyclohexene hydrogenation and cyclohexane dehydrogenation

E2. Gibbs free energy of ethylene hydrogenation and ethane dehydrogenation

Table E2 Gibbs energy of formation [32]

Substance	A	B	C
$C_2H_6(g)$	-85.787	0.16858	0.000026853
$C_2H_4(g)$	51.752	0.049338	0.000017284

$\Delta G_f°$ = A + BT + CT^2 (kJ/mol)

$G_f°[C_2H_6(g)] = (-85.787) + (0.16858)(298.15) + (0.000026853)(298.15)^2$

$G_f°[C_2H_6(g)] = -33.13$ kJ/mol

$G_f°[C_2H_4(g)] = (51.752) + (0.049338)(298.15) + (0.000017284)(298.15)^2$

$G_f°[C_2H_4(g)] = 67.99$ kJ/mol

$G_f°[H_2(g)] = 0$ kJ/mol

$C_2H_6(g) \longrightarrow C_2H_4(g) + H_2(g)$

$\Delta G°_{rxn} = \sum \Delta G_f°_{products} - \sum \Delta G_f°_{reactants}$

$\Delta G°_{rxn} = \{(1\ mol)(G_f°[C_2H_4(g)]) + (1\ mol)(G_f°[H_2(g)])\} - \{(1\ mol)(G_f°[C_2H_6(g)])\}$

$\Delta G°_{rxn} = [(1\ mol)(67.99\ kJ/mol) + (1\ mol)(0\ kJ/mol)] - [(1\ mol)(-33.13\ kJ/mol)]$

$\Delta G°_{rxn} = 101.13$ kJ/mol

ΔG is positive. Therefore, the reaction is not spontaneous.

$C_2H_6(g) \longrightarrow C_2H_4(g) + H_2(g)$

$\Delta G°_{rxn} = \sum \Delta G_f°_{products} - \sum \Delta G_f°_{reactants}$

$\Delta G°_{rxn} = \{(1\ mol)(G_f°[C_2H_6(g)])\} - \{(1\ mol)(G_f°[C_2H_4(g)]) + (1\ mol)(G_f°[H_2(g)])\}$

$\Delta G°_{rxn} = [(1\ mol)(-33.13\ kJ/mol)] - [(1\ mol)(67.99\ kJ/mol) + (1\ mol)(0\ kJ/mol)]$

$\Delta G°_{rxn} = -101.13$ kJ/mol

ΔG is negative. Therefore, the reaction is spontaneous.

The gibbs free energy of c ethylene hydrogenation and ethane dehydrogenation are negative were depicted by :

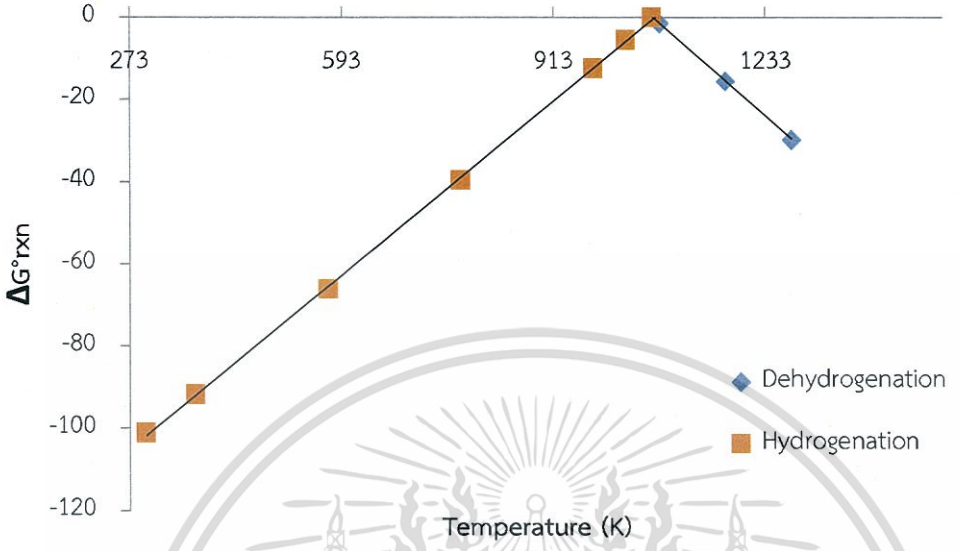

Figure E.2 Gibbs free energy various temperature of ethylene hydrogenation and ethane dehydrogenation

AUTHOR BIOGRAPHY

Name Ms. Teeraporn Kurato
Birth Date July 6, 1994
Birth Place Bangkok, Thailand
Education Year Institution Degree/diploma
2015 King Mongkut's Institute of Technology Ladkrabang Faculty of Science (Chemistry), major in Industrial Chemistry

Name Mr. Satu Kuhatasanadeekul
Birth Date January 3, 1994
Birth Place Bangkok, Thailand
Education Year Institution Degree/diploma
2015 King Mongkut's Institute of Technology Ladkrabang Faculty of Science (Chemistry), major in Industrial Chemistry

Name Mr. Arucha Worathanaseth
Birth Date January 6, 1994
Birth Place Bangkok, Thailand
Education Year Institution Degree/diploma
2015 King Mongkut's Institute of Technology Ladkrabang Faculty of Science (Chemistry), major in Industrial Chemistry